Revision of the crocodilians from the Oligocene of Monteviale, Italy, and the diversity of European eusuchians across the Eocene-Oligocene boundary

Loredana Macaluso, Jérémy Martin, Letizia Del Favero, Massimo Delfino

Revision of the crocodilians from the Oligocene of Monteviale (NE Italy) and the diversity of European eusuchians across the Eocene-Oligocene boundary

LOREDANA MACALUSO,[*,1] JEREMY E. MARTIN,[2] LETIZIA DEL FAVERO,[3] and MASSIMO DELFINO[1,4]

[1] Dipartimento di Scienze della Terra, Via Valperga Caluso 35, 10125, Turin, Italy, macalusoloredana@gmail.com;

[2] Laboratoire de Géologie de Lyon: Terre, Planètes, Environnement, UMR CNRS 5276, Université Lyon 1, Boulevard du 11 Novembre 1918, F-69622 Villeurbanne cedex, France, jeremy.martin@ens-lyon.fr;

[3]Museo di Geologia e Paleontologia, Centro di Ateneo per i Musei, via Giotto 1, 35121, Padova, Italy, letizia.delfavero@unipd.it;

[4]Institut Català de Paleontologia Miquel Crusafont, Universitat Autònoma de Barcelona, Edifici Z (ICTA-ICP), Carrer de les Columnes s/n, Campus de la UAB, E-08193 Cerdanyola del Valles, Barcelona, Spain, massimo.delfino@unito.it

*Corresponding author

ABSTRACT—Crocodilian remains from the Oligocene fossil locality of Monteviale, northeastern Italy, have historically been referred to different genera, but all material was recently assigned to *Diplocynodon* cf. *D. ratelii* Pomel, 1847. The purpose of the present work is to clarify the systematics of the known crocodilian remains from Monteviale. The largest collection is housed in Padua (Italy), but museums in La Rochelle (France), Basel (Switzerland) and London (UK) host crocodilian remains whose uncertain provenance is either Monte Bolca or Monteviale. Radiogenic strontium isotope ratios were measured on the embedding lignite of those specimens to investigate their provenance. The material belongs to the genus *Diplocynodon*, but it clearly differs from *D. ratelii* because the nasal elements are excluded from the extenal nares. *Diplocynodon* from Monteviale shares the same general suture pattern of the skull with the two species *D. tormis* and *D. muelleri. Diplocynodon muelleri* and specimens from Monteviale are also congruent in terms of shape and proportion of the supratemporal fenestrae. However, a revision of *D. muelleri* is currently needed, thus the Monteviale species is identified as *Diplocynodon* cf. *D. muelleri*. In order to examine the relationships of *Diplocynodon* from Monteviale, a phylogenetic analysis was carried out, which does not point to particularly close relationship among *D. muelleri*, *D. tormis*, and the *Diplocynodon* from Monteviale. The occurrence of *Asiatosuchus* in Monteviale is discarded, supporting the hypothesis of a reduction in crocodilian diversity around the Eocene-Oligocene boundary in Europe.

INTRODUCTION

It has been suggested that the composition of the freshwater crocodilian fauna of Europe may have been affected by climatic deterioration around the Eocene-Oligocene boundary (33.9 million years ago; Markwick, 1998; Martin, 2010). Indeed, a marked decline

in diversity is observed between the greenhouse Eocene assemblages, when the European crocodilian fauna is comprised of at least four taxa per locality (with a maximum of seven taxa for Messel; Berg, 1966; Morlo et al., 2004; Hastings, 2017), and the subsequent cooler Oligocene assemblages, wherein each locality hosts the single genus *Diplocynodon*. *Diplocynodon* is therefore thought to have survived dramatic climatic change (see Martin, 2010, for a review).

Italy possesses a rich Cenozoic record of crocodilians (Kotsakis et al., 2004; Delfino et al., 2007; Piras et al., 2007; Abbazzi et al., 2008; Delfino and Rook, 2008; Delfino and Rossi, 2013; Colombero et al., 2017). Among the most famous localities, the lignite deposits from the Eocene of Monte Bolca and the Oligocene of Monteviale have yielded many, often articulated, specimens. Crocodilians from Monte Bolca were attributed to two different taxa by Sacco (1895): *Crocodilus vicetinus* Lioy, 1865, and *Crocodilus bolcensis* Sacco, 1895. The taxonomic affinity of this material is unclear and awaits revision, but there are currently at least three taxa identified: *Asiatosuchus*, *Allognatosuchus* and *Boverisuchus* (Kotsakis et al., 2004). The reported presence of a species of *Diplocynodon* at Monte Bolca (Papazzoni et al., 2014) is erroneous, as the only specimen (MGP-PD 27403) of this genus labelled as coming from this locality is most likely from Monteviale (see below; Del Favero, 1999, Kotsakis et al., 2004). At the beginning of the 20th century, two species from the Oligocene locality of Monteviale were erected: *Crocodilus monsvialensis* Fabiani, 1914, and *Crocodilus dalpiazi* Fabiani, 1915. Fabiani (1914) remarked that *C. monsvialensis* had close affinities with *C. vicetinus* from Monte Bolca, but differed substantially enough to be designated as a new species. Fabiani (1914) briefly listed differences in shape and size of the temporal fenestrae, position of the frontoparietal suture, proportions of the frontal and prefrontal elements, and shape of the nares. Later, Berg (1966:40) proposed that *Diplocynodon* Pomel, 1847, was possibly present at Monte Bolca and Monteviale. He also proposed that some remains from

Monteviale shared the same characters with what he referred to as "*Crocodilus" vicetinus* from Monte Bolca, probably belonging to the same taxon.

The latest comprehensive revisions of the crocodilian assemblage from Monteviale date from the early 1990s. Two taxa were recognized: *Diplocynodon dalpiazi* (Fabiani, 1915) by Franco *et al.* (1992) and *Asiatosuchus monsvialensis* (Fabiani, 1914) by Franco and Piccoli (1993). However, both Rauhe and Rossmann (1995) and Kotsakis et al. (2004) expressed doubts about the presence of two species at Monteviale, suggesting that all these crocodilians belong to a single species of *Diplocynodon* instead. This view was also supported by Brinkmann and Rauhe (1998) in their description of a new specimen from the late Early Oligocene of Céreste, southern France, pertaining to the species *Diplocynodon ratelii* Pomel, 1847. Del Favero (1999) provided a detailed description of the problematic specimen then thought to be from Monte Bolca (MGP-PD 27403), which she referred to *Diplocynodon* cf. *ratelii*. Nannofossils in the matrix surrounding that specimen revealed that it was geologically younger, and therefore from Monteviale. Delfino and Smith (2009) mentioned that the youngest representatives of *Asiatosuchus* could be those from Monteviale if "the referral of '*Crocodilus*' *monsvialensis* (Fabiani, 1914) to crocodyloids by Franco and Piccoli (1993) is valid. Finally, Pandolfi et al. (2016) provided a brief description of the crocodilians from Monteviale, attributing them to a single taxon, *Diplocynodon* cf. *ratelii*.

As shown above, the history of the knowledge of the Monteviale crocodilians is rather convoluted and the precise composition of the assemblage is somewhat still unclear. Although the systematic affinities of these crocodilians have been discussed by various authors, a detailed account of the osteology of the Monteviale crocodilians has yet to be carried out. The works of Franco et al. (1992) and Franco and Piccoli (1993) consist of an exhaustive catalogue of the specimens, but do not include full osteological descriptions based on

diagnostic characters. In this context, the presence of *Asiatosuchus* and *Diplocynodon* in the Oligocene of Monteviale remains to be verified.

We herein provide a detailed osteological description of the Monteviale specimens, housed in the collection of the "Museo Geologia e Paleontologia" of Padua, Italy, and of two previously unreported skeletons housed in the collections of the Musée de La Rochelle, France, and the Naturhistorisches Museum in Basel, Switzerland, that may come from the same locality. This description offers a basis to evaluate the presence of two sympatric taxa in the crocodilian assemblage of Monteviale. We intend to verify if the idea that the diversity of the Oligocene crocodilian assemblage of Italy is really an exception if compared to the European standard, or if the occurrence of *Asiatosuchus* should be discarded, thus confirming the hypothesis of a major reduction in the diversity of crocodilian assemblages around the Eocene-Oligocene boundary.

Ambigous Provenance

The Monteviale origin of the specimens housed in Padua is well confirmed in the catalogues of the museum (except for MGP-PD 27403, most likely from Monteviale labelled as coming from Monte Bolca; see Del Favero, 1999, and Kotsakis et al., 2004). The provenance of the two previously unreported crocodilian skeletons is discussed below. They were donated to the collections of Basel and La Rochelle, where they are currently kept, at the beginning of the 20th century.

The Basel specimen does not bear any label and thus, the knowledge of its provenance is uncertain. The catalogue of entries at the Naturhistorisches Museum in Basel records in 1904 "Bc. 6. *Crocodilus* spec. Vorderer Theil eines Skeletes von oben sichtbar, mit gut erhaltenem Schädel" from the Lower Oligocene of Monte Bolca, this locality being also denoted as Monteviale (L. Costeur, pers. comm. to Jeremy Martin 2007). The crocodilian

skeleton of La Rochelle was purchased for 900 Francs from “Les Fils d’Emile Deyrolle”, a company based in Paris and providing natural history specimens for sale. The acquisition letter mentions a skeleton of *Crocodilus vicetinus* from Monte Bolca and is dated to the 10th of December 1931. The same specimen appears to be advertised in a natural history catalogue “Le Naturaliste” also published by “Les Fils d’Emile Deyrolle” and dated from 1908 (R. Vullo, pers. comm. to Jeremy Martin 2011).

The provenance and age of both specimens is therefore equivocal. The sites of Monte Bolca (middle Eocene) and Monteviale (early Oligocene) are located in the same Italian area, and Monte Bolca was, and still is, much more popular than Monteviale. Confusion about the provenance of fossils from these two localities has always been an issue, and Berg (1966) did not provide any extensive comment on this, just stating that the provenance of *Diplocynodon* from Monte Bolca or Monteviale was unclear. Kotsakis et al. (2004) and Pandolfi et al. (2016) reported that some mammals and crocodilians were likely to have been discovered at Monteviale and then referred by mistake to Monte Bolca. The catalogue of entries in Basel is consistent with such a possibility as the initial name of the locality (Monte Bolca) is crossed and replaced with “Monteviale”. Moreover, the collection is ordered stratigraphically and the crocodilian NMB-Bc.6 and associated mammal material from Monteviale are listed and placed in the upper Rupelian section (and thus among the Oligocene materials, not among the Eocene ones).

The designation of ‘Monte Bolca’ as a locality incorporates various fossiliferous sites of three different depositional environments: Monte Postale and Pesciara di Bolca consisting of micritic limestone deposited in a marine environment (Papazzoni et al., 2014); Spilecco consisting of marly limestones deposited in a shallow water environment (Papazzoni et al., 2014); Purga di Bolca and Vegroni consisting of lignite seams reminiscent of a freshwater depositional environment (Barbieri and Medizza, 1969; Del Favero, 1999). Only the Pesciara

di Bolca benefited from a recent detailed stratigraphic study and a middle Eocene age has been assigned to it (Papazzoni and Trevisani, 2006). An early-middle Eocene age has been proposed for Purga di Bolca (Papazzoni et al., 2014). That the museums of Basel and La Rochelle refer their specimens to Monte Bolca or to *Crocodilus vicetinus* (one of the species described on the basis of material from Monte Bolca) might be due to confusion with Monteviale, or these fossils could genuinely come from lignite sites of Purga di Bolca.

The two crocodilian skeletons from Basel and La Rochelle likely come from Monteviale on the basis of a morphological comparison and the similar encasing matrix of the material with the specimens housed in Padua, which certainly come from Monteviale. However, the assigning of provenance based on these factors is tentative. For this reason, a geochemical analysis comparing the matrix surrounding specimens of known and unknown provenance is presented below.

Institutional Abbreviations—**MLR**, Musée d'Histoire Naturelle de La Rochelle, France; **MGP-PD**, Museo di Geologia e Paleontologia dell'Università di Padova, Italy; **NHM-UK**, Natural History Museum of London, United Kingdon; **NMB**, Naturhistorisches Museum Basel, Switzerland.

MATERIAL AND METHODS

Material

The Monteviale material is subject to degradation connected to pyrite oxidation (see Larkin, 2011). To deal with this problem, during the past century the Padua material has been treated with several varnishes, which covered and obliterated most of the sutures among the bones, making the material very difficult to examine. The specimen housed in the

Naturhistorisches Museum in Basel is the best preserved, as it has been mechanically extracted from the slab and treated with ammonium gas and paraffin to preserve it from pyrite oxidation. The skeleton housed in La Rochelle remains within its original lignite matrix, unprepared in 3D. Most of the material is figured in Appendix 1.

Provenance Analysis

Lignites are sedimentary rocks formed from the aggregation of terrestrial plant material and thus they have a variable content of carbon. The plants that make up lignites grow on soil whose minerals originate from the weathering of substrates. Because geological substrates of different natures have their own radiogenic strontium isotope composition (expressed as $^{87}Sr/^{86}Sr$), so do soils that grow on it as well as associated plant remains and organisms that will feed on these plants, thus reflecting a local strontium isotope value (Graustein, 1989; Blum et al., 2000). The lignites of Purga di Bolca are several million years older (middle Eocene) than the lignites of Monteviale (early Oligocene) (Papazzoni and Trevisani, 2006; Papazoni et al., 2014; Pandolfi et al., 2016) and should possess different geochemical compositions. Therefore, we predict that the radiogenic strontium isotope ratio (expressed as $^{87}Sr/^{86}Sr$) of samples from Purga di Bolca will differ from samples from Monteviale. To test this hypothesis, $^{87}Sr/^{86}Sr$ ratios were measured on two lignite samples from Purga di Bolca as well as on two specimens from Monteviale (MGP26855 and MGP26836). In addition, three samples of uncertain provenance including the two specimens presented above (La Rochelle and Basel), as well as one specimen housed in NHM-UK and labelled as coming from from Purga di Bolca, were analyzed. $^{87}Sr/^{86}Sr$ ratios were measured on a Nu instrument-500 multicollector-ICPMS with a Phoenix laser ablation inlet (Photon-Machines) at the Laboratoire de Géologie de Lyon. We are not aware of reference material for $^{87}Sr/^{86}Sr$ ratio in lignite, so we used a homogenous standard of known strontium isotopic

composition (SRM-1400, Bone Ash) as a bracketing reference for correcting instrumental biases during measurements. The standard SRM-1400 contains 250 p.p.m. of strontium and produces about 3 volts on mass ^{88}Sr on the multicollector ICPMS. The standard SRM 1400 yields an average $^{87}Sr/^{86}Sr$ raw value of 0.71371 ± 0.00526 (2 s.d.), which is comparable to the TIMS value of 0.71310 ± 0.00002 (2 s.d.) (Schweissing and Grupe, 2003). Each sample was ablated three times with a spot diameter of 100 μm.

Phylogenetic Analysis

The Monteviale specimens were scored as a single taxon and included in the data matrix of Martin et al. (2014) for eusuchians, which contained a total of 97 taxa, 98 including the Monteviale crocodilian, and 179 characters (Appendix 2). The matrix was assembled using Mesquite (Maddison and Maddison, 2018). The characters are from Brochu et al. (2012; Appendix 3), which are the same used by Martin et al. (2014). All of the most informative species of *Diplocynodon* part of this data matrix: *Diplocynodon darwini*, *D. deponiae*, *D. hantoniensis*, *D. ratelii*, *D. muelleri*, *D. tormis*, and *D. remensis*. Another analysis was conducted that also included two less complete species of *Diplocynodon*, *D. elavericus* and *D. ungeri*, which were also included in some previous analyses (Martin, 2010; Martin and Gross, 2011; Martin et al., 2014). Replicates of 1000 random addition sequences were performed under TNT (Goloboff et al., 2003), using the traditional search with the TBR algorithm to search for shortest trees. *Bernissartia fagesii* was defined as the outgroup taxon as in Martin et al. (2014).

SYSTEMATIC PALEONTOLOGY

Order CROCODILIA Gmelin, 1789

Suborder EUSUCHIA Huxley, 1875

Superfamily ALLIGATOROIDEA Gray, 1844

Family DIPLOCYNODONTIDAE Hua, 2004

Genus DIPLOCYNODON Pomel, 1847

DIPLOCYNODON CF. D. MUELLERI (Kälin, 1936)

(Figs. 1–7)

Crocodilus monsvialensis Fabiani, 1914:233.

Crocodilus dalpiazi Fabiani, 1915:306.

"*Crocodilus*" *vicetinus* Lioy, 1865: Berg, 1966:58.

Diplocynodon dalpiazi (Fabiani, 1915): Franco et al., 1992:130, figs 2–17, pl. 1–3.

Asiatosuchus monsvialensis (Fabiani, 1914): Franco and Piccoli, 1993:101, figs. 3–12, pl. 1–3.

Asiatosuchus monsvialensis (Fabiani, 1914): Roccaforte et al., 1994:380.

Diplocynodon dalpiazi (Fabiani, 1915): Roccaforte et al., 1994:380.

Diplocynodon (Pomel, 1847): Rauhe and Rossmann, 1994: 84.

Diplocynodon ratelii Pomel, 1847: Brinkman and Rauhe, 1998:307–308.

Diplocynodon cf. *ratelii* Pomel, 1847: Del Favero, 1999:110.

Diplocynodon cf. *ratelii* Pomel, 1847: Pandolfi et al., 2016:13–14, figs. 9–10.

Referred material—See Appendix 1 for a complete description of all the specimens. The material includes the two lectotypes: MGP-PD 26814 (lectotype of *Diplocynodon dalpiazi*) and MGP-PD 26843 (lectotype of *Asiatosuchus monsvialensis*). Besides them, the material housed in Padua includes: eight skulls (MGP-PD 10170, MGP-PD 11407, MGP-PD 28164, MGP-PD 26816 and MGP-PD 26817, (skull and lower jaw of the same individual), MGP-PD 26844, MGP-PD 26845, MGP-PD 26846, MGP-PD 26858); three rostri (MGP-PD

26815, MGP-PD 26850, MGP-PD 26862); nine isolated skull fragments (MGP-PD 8648, MGP-PD 26819, MGP-PD 26835, MGP-PD 26837, MGP-PD 26838, MGP-PD 26842, MGP-PD 26957, MGP-PD 26859, MGP-PD 31998); several disarticulated teeth (MGP-PD 26839); and various postcranial elements (MGP-PD 27999–26854 (a single, fractured slab), MGP-PD 26818, MGP-PD 26820, MGP-PD 26821, MGP-PD 26822, MGP-PD 26823, MGP-PD 26824, MGP-PD 26825 – 26830 (a single, fractured slab), MGP-PD 26826, MGP-PD 26827, MGP-PD 26828, MGP-PD 26829, MGP-PD 26831 - 26832 - 26833 - 26834 (derived from the same individual), MGP-PD 26836, MGP-PD 26840, MGP-PD 26841, MGP-PD 26847, MGP-PD 26848, MGP-PD 26849, MGP-PD 26851, MGP-PD 26852–26853 (a single, fractured slab), MGP-PD 26855, MGP-PD 26856, MGP-PD 31997). Besides the numbered specimens, in the Padua museum there are several specimens without numbers: seven fragments of mandibles and maxillae, more than 40 disarticulated teeth, five slabs with poorly preserved portions of the vertebral column, five isolated vertebrae, seven slabs with fragmentary and disarticulated limbs, and several ribs and osteoderms.

MGP-PD 27403 is the previously mentioned slab labelled "Monte Bolca," but as shown below via provenance analysis, it most likely comes from Monteviale. It contains an almost complete specimen which was described by Del Favero (1999).

NMB-Bc.6 is the anterior half of a skeleton with a complete skull showing its dorsal and ventral surfaces (Fig. 1); this slab also contains two areas (indicated with A and B in Fig. 1), with bones belonging to one or two smaller individuals.

MLR-no number, slab with a skeleton bearing a skull visible in dorsal view and disarticulated and fragmented portion of the postcranial skeleton.

NHM-UK 2789 is slab particularly altered by pyrite oxidation containing the thoracic portion of a small individual and part of its limbs.

Occurrence—Early Oligocene (late Rupelian) of Monteviale, Vicenza, north-eastern Italy (Pandolfi et al., 2016).

Description—Although most of the skulls are generally complete or only partially incomplete, the deformation is so intense that it is not possible to evaluate all those characters needed to establish the degree of inclination or orientation of structures (e.g. the direction of the internal choana or the orientation of the basioccipital under the occipital condyle).

Seven of the ten skulls housed in Padua preserve the lower jaw compressed against the maxilla, covering the maxillary teeth. MGP-PD 10170 is significantly affected by the pyrite oxidation and therefore not informative. Only MGP-PD 26816 preserves the lower jaw (labelled as MGP-PD 26817) isolated from the skull, but due to deformation, the contacts among the bones of the mandible are not perceivable. The best preserved skull is the one reported in Figure 3 in which the suture pattern - at least the dorsal one - can be almost completely reconstructed.

From an overall perspective, the skulls are relatively broad, presenting wide premaxillae, a curved maxillary contour at the level of the largest teeth, and diminutive orbits. However, the rostrum is quite elongate, the interorbital space is relatively narrow and the skull table is not expanded laterally and does not project posteriorly.

The anterior region of the rostrum is massive with an almost straight anterior margin of the premaxillae. The external nares are nearly rectangular, being slightly longer than wide. The external nares are slightly smaller than the orbit. As it is particularly clear in MGP-PD 26862, the posterolateral margin of the nares is elevated and the anterior region of the rim of the nares is flat and continuous with the external margin of the bone. All the skulls and the fragments of rostrum present the same suture pattern, described below. The nasals are clearly excluded from the posterior margin of the nares by the premaxillae as these bones are anteroposteriorly expanded at the level of the premaxillary-maxillary notch. The

premaxillary-maxillary suture is delineated by a pronounced embayment for reception of the third and fourth dentary teeth. At the level of the double caniniform tooth, the lateral maxillary margin is inflated. The nasals extend along most of the rostrum length. They taper anteriorly between the premaxillae, which send a short posterior process between the maxilla and nasal at the level of the first or second maxillary alveoli. The sutural pattern of the antorbital region is obscured in most of the specimens, but in two specimens, reported in Figure 3 and Figure 4 (A, B), which preserve the area clearly, the frontal separates the posterior tips of the nasals. The left side of NMB-Bc.6 indicates that the lacrimal tapers relatively far anteriorly at about the level of the sixth maxillary alveolus and therefore extensively contacts the posterolateral margin of the nasal. The prefrontal is not clearly distinguishable in any of the skulls.

The orbital region is characterized by a narrow interorbital width and small orbits. The anterior projection of the frontal is narrow (Figs 3, 4B). The interorbital region is marked by a well-delineated preorbital ridge passing through the frontal and following the anteromedial margin of the orbits on the prefrontal and lacrimal (Figs 3 and 4C). The interorbital region could seem different in Fig. 3A and Fig. 4C, but the different shape in Fig. 4C is due to a taphonomic effect. In fact, in Fig. 4C the anterior process of the prefrontal is detached and raised from the lacrimals surrounding it. The anterior-most margin of the orbits is formed by the lacrimal and is notched. This notch marks a depression, where the ornamentation is absent. The teardrop-shaped supratemporal fenestrae are well preserved in MGP-PD 28164 (Fig. 5), 26843, 26858 (Fig. 4C) and NMB-Bc.6 (Fig. 3). In NMB-Bc.6 and in MGP-PD 28164, the frontoparietal suture clearly penetrates the supratemporal fenestrae, preventing the postorbital from contacting the parietal on the skull table. The parietal is particularly wide between the supratemporal fenestrae, being almost as wide as each fenestra. The supraoccipital participates in the dorsal surface of the skull table and, even if the anterior part

of its suture with the parietal is not clearly visible in any of the specimens, it surely does not prevent the parietal from reaching the posterior margin of the table. The squamosal prongs are short and do not project far posteriorly nor laterally, as particularly evident in NMB-Bc.6.

The suture organization around the lower temporal fenestra is poorly visible in most of the specimens, because of the deformation they have been subjected to. The lower temporal fenestra seems narrow and elongate, but this may be an artefact of compression. The quadratojugal seems to form the posterior corner of this fenestra and extend along its dorsal margin, therefore excluding the quadrate from it. A small quadratojugal spine can be reconstructed to have been located near the dorsal level of the lower temporal fenestra, but it is not preserved in any specimen. The postorbital bar is barely visible (e.g. in MGP-PD 26814 and in NMB-Bc.6) because it is hidden by other bones due to deformation. The jugal projects far posteriorly, but does not prevent any lateral exposure of the quadratojugal, particularly evident in Figure 3. The small medial quadrate hemicondyle bears the notch for the foramen aëreum on its dorsal surface, as evident in most of the specimens (e.g. MGP-PD 26814, 26816, 26835, NMB-Bc. 6).

The palatal structure cannot be entirely reconstructed. The paired palatines comprise the median walls of the suborbital fenestrae. Their anterior part is never visible and thus the anterior extension of the suborbital fenestrae cannot be understood. The posterior part of the suborbital fenestrae are particularly well preserved in MGP-PD 26858 (Fig. 4D) and partially preserved in NMB-Bc.6. The palatines have parallel margins and there is no lateral flaring of each bone (Fig. 4D). The palatine-pterygoid suture is located well ahead of the posterior corner of the suborbital fenestra (Fig. 4D). The lateral edges of the palatines are parallel posteriorly, without producing a shelf. The pterygoid edge contributing to the posterior rim of the suborbital fenestra does not show any notch. The internal choanae open in the central region of the pterygoids. Their lateral margins form a collar, the pterygoid being depressed

lateral to it (particularly visible in MGP-PD 26844). The anterior extension of the ectopterygoid is unclear. The ventral ectopterygoid process is massive and does not project all the way to the tip of the pterygoid wing. Instead, it stops at more than half the distance, as visible in Figure 6D and NMB-Bc.6.

The mandibles are often associated, and articulated, with the skulls, but because of the strong deformation that they have suffered they are usually opened at the level of the contact between splenial and dentary (so that the external surface of the dentary and the internal surface of the splenial are exposed). Moreover, even if the bones are generally identified, most of the characters important for the identification are unperceivable. For example, the articular elements are very common among the Padua specimens, but the foramen aëreum is in most cases not visible. The mandibular symphysis is often visible – particularly well in Figure 6 (B, C, E, F) – and it extends to the 4th mandibular tooth. The surangular is pinched off anterior to the posterior extent of the retroarticular process in MGP-PD 26814. The retroarticular process is deeply concave and its tip projects posterodorsally.

The total number of teeth cannot be assessed. The maxillary teeth are at least 13 in MGP-PD 26844. When the dental pattern can be reconstructed, it emerges that the largest maxillary alveoli are the 4th and 5th, which are confluent. In MGP-PD 26815 and 26844, the 4th alveolus seems slightly smaller than the 5th (Fig. 2). The implication of this character will be discussed in the next section. The 6th tooth is considerably smaller than the 5th one. The 4th dentary alveolus is the largest, and its tooth is hosted in the notch corresponding to the maxilla-premaxilla suture. Even if the 3rd tooth is not preserved in any specimen, the maxillary notch is wide enough to host two dentary teeth in occlusion, corresponding to the 3rd and 4th confluent dentary alveoli. The occlusion is comparable to that of other species of *Diplocynodon* and can be reconstructed particularly well in MGP-PD 8648. In this specimen,

the maxilla is fractured in the two points in which the maxilla is notched, after the 4th mandibular tooth and after the 7th maxillary tooth.

Limited information can be gained from the postcranial elements. Among the Padua material, there are several portions of postcranial elements, but they are usually poorly preserved, or particularly altered. The vertebral column cannot be entirely reconstructed, because all the remains are fragmentary, and some parts of the vertebral column (i.e. the cervical vertebrae) are poorly preserved. The atlas is only preserved, but disarticulated, in NMB-Bc.6, which also preserves the axis and the third cervical vertebra in lateral view (Fig. 3C). Another axis is preserved (MGP-PD 26856), but its anterior crest is broken in both cases. The limbs and the pelvic and scapular girdle are also very fragmentary, even if in some cases still articulated. These elements were dissociated before burial of the animals as testified by the incompleteness also of NMB-Bc.6, which lacks the posterior trunk region. A similar pattern can be observed in the La Rochelle skeleton where only the left forelimb is still partially articulated and most of the dorsal osteoderms and the trunk vertebrae are missing. Noteworthy is the organization of the dorsal armor in the trunk region of NMB-Bc.6, where neural arches are visible, indicating the midline of the trunk (Fig. 7A, B). Herein is also visible a lateral osteoderm and it is therefore possible to clearly identify where the dorsal osteoderms stop. Each row of dorsal osteoderm can be thus reconstructed as containing six osteoderms (Fig. 7B). The dorsal midline osteoderms bear anterior process (Fig. 7C). The ventral armor is visible in lateral view in Figure 7 (D, E), where the ventral, bipartite osteoderms are clearly visible, and one ischium is also detectable (Fig. 7F). The distal portion of the shaft is greatly expanded; the maximum diameter of this expansion is oblique in position. The entire external surface of the ischium is somewhat convex. Each series of osteoderms overlaps the next series located posterior to it.

RESULTS

Provenance Analysis

Results are presented in Table 1 and Figure 8. The most radiogenic values were measured on the two samples from Purga di Bolca (average = 0.732). These differ significantly from the rest of the samples measured here (average = 0.711), including the two samples from Monteviale (MGP26855 and MGP26836), the samples from Basel and La Rochelle, and surprisingly the sample NHM-UK 2789 originally labelled as coming from Purga di Bolca.

Taxonomic Identification

The specific assignment to *Diplocynodon ratelii* by Brinkmann and Rauhe (1998), Del Favero (1999) and Pandolfi et al. (2016) is not accepted here, as discussed below. The organization of the sutures of the skull is basically the same as *D. tormis* from the Eocene, and *D. muelleri* from the Oligocene, of Spain (Buscalioni et al., 1992; Piras and Buscalioni, 2006). Besides being the same age, *D. muelleri* and the Monteviale crocodilians share the shape and proportions of the skull table, which bears teardrop-like supratemporal fenestrae (for *D. muelleri* see holotype in fig. 3 in Piras & Buscalioni, 2006), whereas in *D. tormis* they are more elliptical (see holotype in fig. 2 in Buscalioni et al., 1992). Moreover, the parietal between them is not as thin as in *D. tormis*, where each fenestra is twice as wide as the parietal. In the Monteviale specimens and *D. muelleri*, the parietal is about the same width as each fenestra. Piras and Buscalioni (2006) stated that *D. muelleri* shows a particularly short mandibular symphysis reaching the third mandibular alveolus. In this respect, the Monteviale specimens differ from it, as the symphysis reaches the fourth alveolus. However, in the holotype of *D. muelleri* (NMB-Spa.4), housed in Basel, the mandible is broken at the level of

the mandibular symphysis and it is therefore impossible to evaluate its extension. In *D. muelleri* NMB-Spa.73, the symphysis does not seem shorter than the one of the Monteviale specimens. A revision of the symphyses of all the specimens of *D. muelleri* is needed, but, at the state of the art, this character is not considered sufficient to distinguish between the Spanish species of *Diplocynodon* and the Monteviale crocodilian. The maxillary dentition pattern can be reconstruced only in two specimens from Monteviale (MGP-PD 26844 and MGP-PD 26815), which show the typical confluent 4^{th} and 5^{th} alveoli, but, differently from the other species of *Diplocynodon*, the 4^{th} alveolus seems slightly smaller than the 5^{th} (Fig. 2). Even if this character state is also found in *Asiatosuchus*-like crocodyloid taxa, the rest of the anatomy agrees with placement of these specimens in *Diplocynodon*. However, this feature could be only due to intraspecific variability and it seems more cautious to not consider it significant enough to attribute the material to a species separate from the others.

Phylogenetic Analysis

As in Martin et al. (2014), two analyses were carried out: including the two less complete species of *D. ungeri* and *D. elavericus* and excluding them. The topology and the nodal support metrics are in both cases consistent with the results of Martin et al. (2014). The *Diplocynodon* group has a Bremer (decay) index of one, but it is supported by seven unambigous synaphomorphies (characters 14, 33, 41, 68, 81, 148, 152 of Brochu et al., 2012). As in Martin et al. (2014), including the less complete species, the tree shows a polytomy at the basis of Diplocynodontidae (topology not reported herein), leaving unresolved the relationships among its members. The analysis excluding the less complete species retained 640 trees [consistency index (CI) = 0.3412; retention index (RI) = 0.8021]. For clarity of reading, the strict consensus tree excluding the less complete species (Fig. 9) has been simplified for some clades (i.e. Gavialoidea, Globidonta, and Crocodyloidea). The Monteviale

species is placed in a derived position, in a polytomy with *D. tormis* and *D. muelleri*, that is the sister group of *D. ratelii*.

DISCUSSION

Provenance Analysis

The present geochemical approach relies on a comparative assessment of the radiogenic strontium isotope values of two lignites from two localities. The $^{87}Sr/^{86}Sr$ composition of lignites for provenance purposes has not been widely used in paleontology and heterogeneity of the lignites may be problematic. Nevertheless, values obtained in the sample size available to fall into two groups. Our small sample size precludes statistical analysis. The strontium isotope values measured in the sediment depend on the age and lithology of the bedrock source. The high ratios measured in Purga di Bolca samples indicate a highly radiogenic source, possibly an old granitic substrate. On the other hand, the lignite from Monteviale was sourced from bedrock of a different composition. Results show that the lignite matrix surrounding the crocodile specimens housed in the Musée de La Rochelle, NMB Basel and NHM-UK London have strontium isotope ratios comparable to the samples analyzed from the Oligocene locality of Monteviale. It seems reasonable to consider these specimens as originating from Monteviale unless further analyses show otherwise.

Affinities of the Oligocene Crocodilians from Monteviale

After the revision of all the available crocodilian remains, it is clear that the Monteviale material belongs to a single species of *Diplocynodon*, as previously suggested (Rauhe and Rossmann, 1995; Kotsakis et al., 2004; Pandolfi et al., 2016). In fact, it shares the diagnostic characters of this genus: anterior process of the dorsal osteoderms, bipartite ventral

osteoderms (Fig. 7E), a pair of caniniform teeth hosted in confluent alveoli (maxillary teeth 4 and 5; Fig. 2), and the presence of a preorbital ridge (Fig. 3; Martin et al., 2014). This differs from *Asiatosuchus*-like crocodyloid taxa, which have a single enlarged fifth maxillary tooth and lack the preorbital ridge and the bipartite, ventral osteoderms (Delfino and Smith, 2009). Also, while both the Monteviale species of *Diplocynodon* and *Asiatosuchus* have small orbits compared to their skull size, the interorbital width in *Asiatosuchus* is much larger. The position of the frontoparietal suture does not seem to discriminate any affinity. In species of *Diplocynodon* and *Asiatosuchus germanicus*, the suture makes a deep entry in the supratemporal fenestra (Brochu, 1999) whereas in *A. grangeri* and *Asiatosuchus depressifrons*, the suture lies entirely on the skull table (Delfino and Smith, 2009; but see also Delfino et al., 2017, for the morphology of the oldest European *Asiatosuchus*). In the Monteviale specimens the suture makes a deep entry in the supratemporal fenestrae, a condition currently unknown in *Asiatosuchus* spp. The position of the foramen aëreum observed in the Monteviale species of *Diplocynodon* differs from that of *Asiatosuchus* and *Asiatosuchus*-like taxa for which the foramen aëreum is medially shifted. Here, this foramen is placed on the dorsal surface of the quadrate.

In *Asiatosuchus* the mandibular symphysis is long, extending at least to the sixth dentary alveolus (Leriche, 1899; Mook, 1940; Berg, 1966; Vasse, 1992; Delfino and Smith, 2009; Delfino et al., 2017). On the contrary, in species of *Diplocynodon* the symphysis extends between the third and the fourth dentary alveoli and is therefore shorter. The morphology exhibited by all the skulls from Monteviale clearly shows the condition found in species of *Diplocynodon*, extending the dentary symphysis to the fourth alveolus (e.g., MGP-PD 26843, MGP-PD 26844, MGP-PD 26814, MGP-PD 26815). The 3rd and 4th dentary alveoli, which are confluent in the species of *Diplocynodon*, are not visible in any case, but the corresponding maxillary notch is wide enough to host two teeth. The marked

premaxillary-maxillary notch is not diagnostic for *Asiatosuchus*, as it is present in several species of *Diplocynodon*. This feature develops during ontogeny, as observed for *D. hantoniensis* (Owen, 1849; Norell et al., 1994), *D. ratelii* (Berg, 1966; Brochu, 1999), *D. muelleri* (Piras and Buscalioni, 2006) and probably for most other species of *Diplocynodon*.

From a strictly osteological comparisons, there is no reason to support the option that *Asiatosuchus* was present at Monteviale (Franco and Piccoli, 1993) and the morphological uniformity of all the available material indicates that only one taxon is present. In fact, specimens which are only represented by anatomical elements not preserved on the types of *D. muelleri* or which, for preservational reasons, do not bear any diagnostic character are tentatively referred to the only species present in Monteviale, because they do not differ in morphology and size from *Diplocynodon*. This is also confirmed by the phylogenetic analysis which places the Monteviale crocodilian in a derived position nested among the other species of *Diplocynodon*. Indeed, all the remains from Monteviale presented in the literature should be ascribed to the genus *Diplocynodon*. This observation is also consistent with the known stratigraphic range of the genus *Asiatosuchus*, the latest unambiguous occurrence of which is from the Late Eocene (Bartonian) of Camburg, Germany (Vasse, 1992).

As far as the specific assignment is concerned, the previous specific attribution to *D. ratelii* (Brinkmann and Rauhe, 1998) and *D.* cf. *ratelii* (Pandolfi et al., 2016) is not confirmed. In fact, in *D. ratelii* the nasals clearly reach the external nares (Díaz Aráez et al., 2017), whereas in the studied material the nasals stop at least one centimetre away from the nares (Figs 3B, 4B, 5B). This is also confirmed by the phylogenetic analysis carried out, which retrieved the Monteviale specimen in a polytomy with the two Spanish species of *D. tormis* (Buscalioni et al., 1992) and *D. muelleri* (Piras and Buscalioni, 2006), forming together the sister group of *D. ratelii*. The morphology and the suture organization are very similar to those of *D. tormis* and *D. muelleri*. *Diplocynodon tormis* is an alligatoroid found in

the Eocene of Iberia (Buscalioni et al., 1992), whereas *D. muelleri* comes from the Oligocene of the same area (Piras and Buscalioni, 2006). These two species are very similar, showing no difference in the suture pattern of the skull. The general shape of the skull is asserted to be different by Piras and Buscalioni (2006), but this difference is most likely due to the fact that *D. muelleri* is dorso-ventrally compressed because of taphonomic processes, in a similar way of the *Diplocynodon* of Monteviale, whereas *D. tormis*, not being dorsoventrally compressed on a slab, preserved better the three-dimensional aspect of the skull, seeming slender. The main differences pointed out by Piras and Buscalioni (2006) concern the mandibular symphysis which they describe as particularly short in *D. muelleri*, reaching the third mandibular alveolus, and the palatal fenestrae which are described as particularly long in *D. muelleri*. Actually, a direct analysis of the *D. muelleri* holotype (NMB-Spa 4 T2) and another specimen (NMB-Spa 73) of this species, which are housed in Basel, indicated that these differences are not so evident. In fact, the holotype does not preserve the symphysis which is broken off and its palatal fenestrae are not clearly separated from the rest of the skull. The palatal fenestrae show a similar condition in NMB-Spa 73, but the symphysis is preserved and does not seem significantly less extended than in the Monteviale specimens, in which it reaches the 4th mandibular alveolus. Another difference between *D. muelleri* and *D. tormis* is realated to the shape and proportion of the supratemporal fenestrae. The supratemporal fenestrae in *D. tormis*, in fact, are elliptical and wide, being twice as wide as the parietal between them, whereas in *D. muelleri*, they have a more teardrop-like shape and the parietal is wider between them. In this respect, the Monteviale specimens are more similar to *D. muelleri* than to *D. tormis*. Indeed, the supratemporal fenestrae are teardrop-like and the parietal is as wide as the fenestrae, as in *D. muelleri*. However, the skull table and the supratemporal fenestrae are known to change during ontogeny (Iordansky, 1973) and for this reason they are not widely used as important characters for taxonomy and phylogeny (Brochu,

1999). A careful revision of the species *D. tormis* and *D. muelleri* is currently needed to confirm the validity of both species ; indeed they may represent the same species at different ontogenetic stages. Currently, the Monteviale alligatoroid can be considered more similar to *D. muelleri* than to *D. tormis*.

Implications for Crocodilian Turnover

Comparative osteology suggests that no evidence exists for the presence of crocodyloids in the late Early Oligocene of Monteviale. Several European Eocene localities include multiple species within a given environment (Markwick, 1998; Martin, 2010). One hallmark example is the Messel oil shale locality (early Middle Eocene, MP 11, ca. 47 M.a.), which is composed of two generalist taxa of different size (the alligatoroid *Diplocynodon darwini* and the crocodyloid '*Asiatosuchus*' *germanicus*), one or two terrestrial predators (the sebecid *Bergisuchus dietrichbergi* and the eusuchian *Boverisuchus rollinati*), and a diminutive tribodont (*Hassiacosuchus haupti*). This diverse assemblage thrived under the greenhouse climate during part of the Eocene. But climatic conditions drastically changed near the end of the Eocene (Zachos et al., 2001, Mosbrugger et al., 2005; Escarguel et al., 2008; Héran et al., 2010); the progressive development of cooler conditions and the marked temperature decline at the very end of the Eocene most probably influenced the distribution of ectothermic taxa and contributed to the diversity decline observed across the EOB in crocodilian assemblages. After this event, the continental fossil record indicates only the presence of species of *Diplocynodon* (Antunes and Cahuzac, 1999; Piras et al., 2007). Due to their physiological constraints, crocodilians have been used as climatic proxies for inferring the latitudinal gradient of temperatures and hygrometry in the past (Markwick, 1998). Our results confirm this pattern: only one species exists in the Oligocene of Monteviale, namely a

species of *Diplocynodon*, a taxon broadly encountered in the freshwater ecosystems of that epoch.

CONCLUSIONS

The radiogenic strontium isotope ratio analysis performed herein revealed itself successfull in ascertaining the provenance of the three previously unreported specimens *Diplocynodon* housed in collections in Basel, La Rochelle and London. This method can perhaps be applied to other specimens in general, and in particular to those specimens coming from north-east of Italy whose provenance is uncertain.

Following the morphological and taxonomic revision of all the available material, the crocodilians from Monteviale are assigned to a single species of the genus *Diplocynodon*, as previously proposed. There is indeed no evidence of *Asiatosuchus*-like taxa from the Oligocene of Monteviale, thus confirming a stratigraphic range for *Asiatosuchus*-like taxa restricted to the lower side of the Eocene-Oligocene boundary. Moreover, it seems likely that the only problematic specimen of *Diplocynodon* labelled as coming from Monte Bolca is actually coming from Monteviale. In fact, as said above, previous studies already underlined that nannofossils of the matrix of this specimen indicated a younger age than Eocene, compatible with Oligocene of Monteviale (Del Favero, 1999; Kotsakis et al., 2004). Furthermore, after our study, the morphological similarity between this single specimen labelled as coming from Monte Bolca and the Monteviale crocodilian is clear and thus the presence of a species of *Diplocynodon* in Monte Bolca seems to be unsubstantiated. The specific attribution *Diplocynodon* cf. *D. muelleri* is proposed, but a revision of the potential synonymy of the two Spanish species, *D. tormis* from the Eocene and *D. muelleri* from the Oligocene, is currently needed.

ACKNOWLEDGMENTS

LM thanks A. Borrani for the help during the phylogenetic analysis with TNT, S. Maidment for access to the NHMUK collections, and P. Mannion and C. Nicholl for assistance. LM visited NHMUK thanks to an Erasmus Traineeship at the Imperial College of London (under the supervision of P. Mannion). JEM thanks E. Buffetaut and J-M. Mazin for reading an early version; JEM also thanks P. Telouk at LGLTPE for his help in setting up the laser ablation facilities. S. Salisbury provided comments on an earlier draft of this manuscript. Michael D'Emic, Daniela Schwarz and an anonymous reviewer greatly enhanced the quality of a former version of this work through constructive comments. JEM thanks the curators who provided lignite samples for analysis: L. Costeur (Basel), J-F. Heil (La Rochelle), R. Vullo (La Rochelle), M. Fornasiero (Padua), R. Zorzin (Verona) and L. Steel (NHM-UK, London).

REFERENCES

Abbazzi, A., M. Delfino, G. Gallai, L. Trebini, and L. Rook. 2008. New data on the vertebrate assemblage of Fiume Santo (North-West Sardinia Italy) and overview on the Late Miocene Tusco-Sardinian palaeobioprovince. Palaeontology 52:251–425.

Antunes, M. T., and B. Cahuzac. 1999. Crocodilian faunal renewal in the upper Oligocene of Western Europe. Comptes rendus de l'Académie des Sciences Paris, Science de la Terre et des planètes 328:67–73.

Barbieri, G., and F. Medizza. 1969. Contributo alla conoscenza geologica della regione di Bolca (Monti Lessini). Memorie dell'Istituto di Geologia e Mineralogia dell'Università di Padova 27:1–36.

Berg, D. E. 1966. Die Krokodile, insbesondere *Asiatosuchus* und aff. *Sebecus*?, aus dem Eozän von Messel bei Darmstadt/Hessen. Abhandlungen des Hessischen Landesamtes für Bodenforschung 52:1–105.

Blum, J. D., E. H. Taliaferro, M. T. Weisse, and R. T. Holmes. 2000. Changes in Sr/Ca, Ba/Ca and $^{87}Sr/^{86}Sr$ ratios between trophic levels in two forest ecosystems in the northeastern U.S.A. Biochemistry 49:87–101.

Brinkmann, W., and M. Rauhe. 1998. *Diplocynodon ratelii* Pomel, 1847 (Crocodylia, Leidyosuchidae) aus dem unter–Oligozän von Céreste (Südfrankreich). Neues Jahrbuch für Paläontologie Abhandlungen 209:295–321.

Brochu, C. A. 1999. Phylogeny, systematics, and historical biogeography of Alligatoroidea. Society of Vertebrate Paleontology Memoir 6:9–100.

Brochu, C. A., D. C. Parris, B. S. Grandstaff, R. K. Denton Jr, and W. B. Gallagher. 2012. A new species of *Borealosuchus* (Crocodyliformes, Eusuchia) from the Late Cretaceous–early Paleogene of New Jersey. Journal of Vertebrate Paleontology 32(1):105–116.

Buscalioni, A. D., J. L. Sanz, and M. L. Casanovas. 1992. A new species of the eusuchian crocodile *Diplocynodon* from the Eocene of Spain. Neues Jahrbuch für Geologie und Paläontologie Abhandlungen 187:1–29.

Colombero, S., D. M. Alba, C. D'amico, M. Delfino, D. Esu, P. Giuntelli, M. Harzhauser, P. P. A. Mazza, M. Mosca, T. A. Neubauer, G. Pavia, M. Pavia, A. Villa, and **G.** Carnevale. 2017. Late Messinian mollusks and vertebrates from Moncucco Torinese, north-western Italy. Paleoecological and paleoclimatological implications. Palaeontologia Electronica 20.1.10A:1–66.

Del Favero, L. 1999. Un esemplare di *Diplocynodon* Pomel, 1847 (Crocodylia, Leidyosuchidae) conservato nel museo geopaleontologico dell' Università di Padova. Lavori Società Veneta di Scienze Naturali 24:107–117.

Delfino, M., and L. Rook. 2008. African crocodylians in the Late Neogene of Europe. A revision of *Crocodylus bambolii* Ristori, 1890. Journal of Paleontology 82:336–343.

Delfino, M., and T. Smith. 2009. A reassessment of the morphology and taxonomic status of '*Crocodylus*' *depressifrons* Blainville, 1855 (Crocodylia, Crocodyloidea) based on the Early Eocene remains from Belgium. Zoological Journal of the Linnean Society of London 156:140–167.

Delfino, M., and M. A. Rossi. 2013. Fossil crocodylid remains from Scontrone (Tortonian, Southern Italy) and the late Neogene Mediterranean biogeography of crocodylians. Geobios 46:25–31.

Delfino, M., M. Böhme, and L. Rook. 2007. First European evidence for transcontinental dispersal of *Crocodylus* (late Neogene of southern Italy). Zoological Journal of Linnean Society 149:239–307.

Diaz Araez, J. L., M. Delfino, À. H. Lujan, J. Fortuny, F. Bernardini, and D. M. Alba. 2017. New remains of *Diplocynodon* (Crocodylia: Diplocynodontidae) from the Early Miocene of the Iberian Peninsula. Comptes Rendus Palevol 16:12–26.

Escarguel, G., S. Legendre, and B. Sigé. 2008. Unearthing deep–time biodiversity changes: The Palaeogene mammalian metacommunity of the Quercy and Limagne area (Massif Central, France). Comptes Rendus Geoscience 340:602–614.

Fabiani, R. 1914. La serie stratigrafica del Monte Bolca e dei suoi dintorni. Memorie dell'Istituto Geologico della R. Università di Padova 2 :223–235.

Fabiani, R. 1915. Il Paleogene del Veneto. Memorie dell'Istituto Geologico della R. Università di Padova 3:1–336.

Franco, R., and G. Piccoli. 1993. A small crocodilian species from the Oligocene of Monteviale in Vicentinian, *Asiatosuchus monsvialensis* (Fabiani, 1914). Memorie di Scienze Geologiche, Padova 45:99–114.

Franco, R., G. Piccoli, and M. Tchaprassian. 1992. Resti di coccodrilli Diplocynodonti (*Diplocynodon dalpiazi*) dall'Oligocene di Monteviale (Vicenza) nel Museo Paleontologico Universitario di Padova. Memorie di Scienze Geologiche, Padova 44:127–149.

Gmelin, J. 1789. Linnei Systema Naturae. Beer, G. E. (ed.), Leipzig, 1057 pp.

Gray, J. E. 1844. Catalogue of the tortoises, crocodiles, and amphisbaenians in the collection ofthe British Museum. Trustees of the British Museum, London.

Goloboff, P. A., J. S. Farris, and K. Nixon. 2003. TNT: tree analysis using new technologies. Program and documentation available from the authors and at: http://www.zmuc.dk/public/phylogeny

Graustein, W. C. 1989. $^{87}Sr/^{86}Sr$ ratios measure the sources and flow of strontium in terrestrial ecosystems. Pp. 491–512 in Stable isotopes in ecological research, Springer-Verlag.

Hastings, A. K. 2017. Terrestrial Conservation Lagerstätten: Windows into the Evolution of Life on Land. Fraser, N. C., and H.-D. Sues (eds). Dunedin Academic Press, 450 pp.

Héran, M. A., C. Lécuyer, and S. Legendre. 2010. Cenozoic long–term terrestrial climatic evolution in Germany tracked by $\delta^{18}O$ of rodent tooth phosphate. Palaeogeography, Palaeoclimatology, Palaeoecology 285:331–342.

Hua, S. 2004. Les crocodiliens du Sparnacien (Eocène inférieur) du Quesnoy (Oise, France). Oryctos 5:57–62.

Huxley, T. H. 1875. On *Stagonolepis Robertsoni*, and on the evolution of the Crocodilia. Quaterly Journal of the Geological Society of London 3:423–438.

Iordansky, N. N. 1973. The skull of the Crocodilia. Biology of the Reptilia 4:201–262.

Kälin, J. A. 1936. *Hispanochampsa mülleri* nov. gen. nov. spec., ein neuer Crocodilide aus dem unteren Oligocaen von Tárrega (Catalonien). Abhandlungen Schweizerischen Palaeontologischen Gesellschaft 58:1–40.

Kotsakis, T., M. Delfino, and P. Piras. 2004. Italian Cenozoic crocodilians: taxa, timing and biogeographic implications. Palaeogeography, Palaeoclimatology, Palaeoecology 210:67–87.

Larkin, N. R. 2011. Pyrite Decay: cause and effect, prevention and cure. Natural Science Collections Association News 21:35–43.

Leriche, M. 1899. Note sur le *Crocodilus depressifrons* trouvé à Urcel (Aisne). Annales de la Société Géologique du Nord 38:92–94.

Lioy, P. 1865. Cenni sopra uno scheletro completo di coccodrillo fossile scoperto in Monte Purga di Bolca *Crocodilus vicetinus*. Atti della Societa Italiana di Scienze Naturali 8:393–397.

Maddison, W. P., and D. R. Maddison. 2018. Mesquite: a modular system for evolutionary analysis. Version 3.51 http://www.mesquiteproject.org

Markwick, P. J. 1998. Fossil crocodilians as indicators of Late Cretaceous and Cenozoic climates: implications for using palaeontological data in reconstructing palaeoclimate. Palaeogeography, Palaeoclimatology, Palaeoecology 137:205–271.

Martin, J. E. 2010. A new species of *Diplocynodon* (Crocodylia, Alligatoroidea) from the Late Eocene of the Massif Central, France, and the evolution of the genus in the climatic context of the Late Palaeogene. Geological Magazine 147:596–610.

Martin, J. E., and M. Gross. 2011. Taxonomic clarification of *Diplocynodon* Pomel, 1847 (Crocodilia) from the Miocene of Styria, Austria. Neues Jahrbuch für Geologie und Paläontologie – Abhandlungen 261:177–193.

Martin, J. E., T. Smith, F. Lapparent de Broin, F. Escuillié, and M. Delfino. 2014. Late Palaeocene eusuchian remains from Mont de Berru, France, and the origin of the alligatoroid *Diplocynodon*. Zoological Journal of the Linnean Society 172:867–891.

Mook, C. C. 1940. A new fossil crocodilian from Mongolia. American Museum Novitates 1097:1–3.

Morlo, M., S. Schaal, G. Mayr, and C. Seiffert. 2004. An annotated taxonomic list of the Middle Eocene (MP11) vertebrata of Messel. Courier Forschungsinstitut Senckenberg 252:95–108.

Mosbrugger, V., T. Utescher, and D. L. Dilcher. 2005. Cenozoic continental climatic evolution of Central Europe. Proceedings of the National Academy of Science 102:14964–14969.

Norell, M. A, J. M. Clark, and J. H. Hutchison. 1994. The Late Cretaceous allligatorid *Brachychampsa montana* (Crocodylia): new material and putative relationships. American Museum Novitates 3116:1–26.

Owen, R. 1849. Fossil Reptilia of the London clay. Part II–Crocodilia and Ophidia. Palaeontographical society monograph, London, 442 pp.

Pandolfi, L., G. Carnevale, L. Costeur, L. Del Favero, M. Fornasiero, E. Ghezzo, L. Maiorino, P. Mietto, P. Piras, L. Rook, G. Sansalone, and T. Kotsakis. 2016. Reassessing the earliest Oligocene vertebrate assemblage of Monteviale (Vicenza, Italy). Journal of Systematic Palaeontology 15(2):83–127.

Papazzoni, C. A., and E. Trevisani. 2006. Facies analysis, palaeoenvironmental reconstruction, and biostratigraphy of the “Pescaria di Bolca” (Verona, northern Italy): an early Eocene Fossil–Lagerstätte. Palaeogeography, Palaeoclimatology, Palaeoecology 242:21–35.

Papazzoni, C. A., L. Giusberti, G. Carnevale, G. Roghi, D. Bassi, and R. Zorzin. 2014. The Bolca Fossil–Lagerstatten: A window into the Eocene World. Rendiconti della Società Paleontologica Italiana 4:1–110.

Piras, P., and A. D. Buscalioni. 2006. *Diplocynodon muelleri* comb. nov., an Oligocene diplocynodontine alligatoroid from Catalonia (Ebro Basin, Lleida province, Spain). Journal of Vertebrate Paleontology 26:608–620.

Piras, P., M. Delfino, L. Del Favero, and T. Kotsakis. 2007. Phylogenetic position of the crocodylian *Megadontosuchus arduini* (de Zigno, 1880) and tomistomine palaeobiogeography. Acta Palaeontologica Polonica 52:315–328.

Pomel, A. 1847. Note sur des animaux fossiles découverts dans le département de l'Allier. Bulletin de la Société Géologique 4:378–385.

Rauhe, M., and T. Rossmann. 1995. News about fossil crocodiles from the Middle Eocene of Messel and Geiseltal, Germany. Hallesches jahrbuch für geowissenschaften B 17:81–92.

Ride, W. D. L., H. G. Cogger, C. Dupuis, O. Kraus, A. Minelli, F. C. Thompson, and P. K. Tubbs. 1999. International Code of Zoological Nomenclature, ed. 4. London: International Trust for Zoological Nomenclature.

Roccaforte, P., G. Piccoli, and L. Sorbini. 1994. The fossiliferous sites with Tertiary vertebrates in Northeastern Italy. Memorie di Scienze Geologiche, Padova 46:373–400.

Sacco, F. 1895. I coccodrilli del Monte Bolca. Memorie della Rale Accademia delle Scienze di Torino, série II 45:75–88.

Schweissing, M. M., and G. Grupe. 2003. Tracing migration events in man and cattle by stable strontium isotope analysis of appositionally grown mineralized tissue. International Journal of Osteoarchaeology 13(1–2):96–103.

Vasse, D. 1992. Un crâne d'*Asiatosuchus germanicus* du Lutétien d'Issel (Aude). Bilan sur le genre *Asiatosuchus* en Europe. Géobios 25 :293–304.

Zachos, J. C., M. Pagani, L. C. Sloan, and K. Billups. 2001. Trends, rhythms, and aberrations in global climate 65 Ma to present. Science 292:686–693.

Submitted Month DD, YYYY; accepted Month DD, YYYY.

FIGURE CAPTIONS

FIGURE 1. The Basel specimens of *Diplocynodon* from the Oligocene of Italy (NMB-Bc.6). **A** and **B** are two areas with some skeletal elements of one or two smaller individuals. Scale bar 5 cm. [planned for page width]

FIGURE 2. Details of the 4th and 5th maxillary alveoli of *Diplocynodon* from the Oligocene of Italy: MGP-PD 26844 (**A**,**B**) and MGP-PD 26815 (**C**,**D**). The two alveoli are confluent, but the 4th seems smaller than the 5th. Scale bar 1 cm. [planned for 2/3 of a whole page width]

FIGURE 3. Skull of *Diplocynodon* from the Oligocene of Italy: NMB-Bc.6 in dorsal view. **A**, dorsal view. **B**, interpretative drawing. **C**, interpretative drawing of the cervical area. **D**, interpretative drawing of the skull table. Scale bar 5 cm. **Abbreviations**: **Ax**, axis; **Ac**, axis crest; **Co**, occipital condilum; **Ex**, exoccipital; **Fr**, frontal; **Ic**, intercentrum; **Ju**, jugal; **Lna**, left neural arc; **Ma**, maxilla; **Na**, nasal; **Pa**, parietal; **Pm**, premaxilla; **Po**, postorbital; **SO**, supraoccipital; **Sq**, squamosal; **Qj**, quadratojugal; **Qu**, quadrate; **Rna**, right neural arch; **Tv**, third cervical vertebra. [planned for 2/3 of a whole page width]

FIGURE 4. Selection of skulls of *Diplocynodon* from the Oligocene of Italy. **A**, MGP-PD 26850 in dorsal view. **B**, interpretative drawing of MGP-PD 26850. **C**, MGP-PD 26858 in dorsal view. **D**, interpretative drawing of the ventral view of MGP-PD 26858, showing the palatines (**Pa**) with parallel margins and the suture between palatines and pterygoids (**Pt**) located well ahead of the posterior corner of the suborbital fenestra. Scale bar 2 cm. **Abbreviations**: **Fr**, frontal; **Ma**, maxilla; **Na**, nasal; **Pm**, premaxilla. [planned for 2/3 of a whole page width]

FIGURE 5. *Diplocynodon* from the Oligocene of Italy. **A**, MGP-PD 28164 in dorsal view. **B**, interpretative drawing of the rostrum. **C**, interpretative drawing of the skull table. Scale bar 1 cm. **Abbreviations**: **Fr**, frontal; **Ma**, maxilla; **Na**, nasal; **Pa**, parietal; **Pm**, premaxilla; **Po**, postorbital; **Sq**, squamosal. [planned for 2/3 of a whole page width]

FIGURE 6. *Diplocynodon* from the Oligocene of Italy. **A**, MGP-PD 26843 in dorsal view. **B**, MGP-PD 26843 in ventral view. **C**, interpretative drawing of the mandibular symphysis of MGP-PD 26843. **D,** right pterygoid wing in ventral view (MGP-PD 31998) showing the contact between pterygoid (**Pt**) and ectopterygoid (**Ec**). **E**, MGP-PD 26815 in ventral view. **F**, interpretative drawing of the mandibular symphysis of MGP-PD 26815. Scale bar 2 cm. [planned for 2/3 of a whole page width]

FIGURE 7. *Diplocynodon* from the Oligocene of Italy. **A**, dorsal armor of NMB-Bc.6. **B**, interpretative drawing of the dorsal armor of NMB-Bc.6, showing that each row of it was composed by three osteoderms per side, so six osteoderms in total. **C**, dorsal osteoderm from NMB-Bc.6, with the typical anterior process. **D**, part of a lombar column (MGP-PD 27999 and 26854) with ventral osteoderms. **E**, detail and interpretative drawing of a ventral, bipartite osteoderm from MGP-PD 27999. **F**, detail of an ischium from MGP-PD 27999. Scale bar 5 cm. [planned for 2/3 of a whole page width]

FIGURE 8. Comparison of strontium isotope ratios ($Sr^{87/86}$) of selected lignites sampled in the embedding matrix of crocodilian skeletons housed in various institutions. [planned for column width]

FIGURE 9. Strict consensus tree resulting from the inclusion of the *Diplocynodon* from Monteviale, Italy in the character matrix of Martin *et al.* (2014). The Monteviale taxon is placed in a derived position within the clade of *Diplocynodon* in a polytomy with *D. muelleri* and *D. tormis*. [planned for column width]

TABLE 1. Strontium isotope ratios (87/86) of selected lignites sampled in the embedding matrix of crocodilian skeletons housed in various institutions.

Provenance	Sample	Mean $^{87}Sr/^{86}Sr$	2SD
unknown	NHM Basle	0,709	0,001
unknown	La Rochelle	0,714	0,003
unknown	NHMUK PRV 2789	0,710	0,002
Monteviale	MGP26855	0,709	0,002
Monteviale	MGP 26836	0,710	0,002
Purga di Bolca	1	0,734	0,008
Purga di Bolca	2	0,731	0,007

Revision of the crocodilians from the Oligocene of Monteviale (NE Italy) and the diversity of European eusuchians across the Eocene-Oligocene boundary

LOREDANA MACALUSO,[*,1] JEREMY E. MARTIN,[2] LETIZIA DEL FAVERO,[3] and MASSIMO DELFINO[1,4]

[1] Dipartimento di Scienze della Terra, Via Valperga Caluso 35, 10125, Turin, Italy, macalusoloredana@gmail.com;

[2] Laboratoire de Géologie de Lyon: Terre, Planètes, Environnement, UMR CNRS 5276, Université Lyon 1, Boulevard du 11 Novembre 1918, F-69622 Villeurbanne cedex, France, jeremy.martin@ens-lyon.fr;

[3]Museo di Geologia e Paleontologia, Centro di Ateneo per i Musei, via Giotto 1, 35121, Padova, Italy, letizia.delfavero@unipd.it;

[4]Institut Català de Paleontologia Miquel Crusafont, Universitat Autònoma de Barcelona, Edifici Z (ICTA-ICP), Carrer de les Columnes s/n, Campus de la UAB, E-08193 Cerdanyola del Valles, Barcelona, Spain, massimo.delfino@unito.it

*Corresponding author

APPENDIX 1.

The material from Padua is described first and subdivided among: (i) complete (or nearly so) skulls, (ii) variably isolated skull elements, and (iii) postcranial elements.

As the Basel, La Rochelle, and London specimens are basically large slabs on which there are whole parts of the individuals, they will be described at the bottom of this section, after the material of Padua. The skeleton housed in the Musée d'Histoire Naturelle of La Rochelle, France is almost complete and gives a good idea of the total length of the animal, although several parts of the postcranial skeleton are not preserved. The skull is complete and visible in dorsal view.

Complete skull

MGP−PD 10170

This catalogue number refers to a skull completely destroyed by the pyrite oxidation. It is now represented by several indistinguishable fragments.

MGP−PD 28164

This catalogue number refers to an almost complete compressed skull with the lower jaw in ventral view (Fig. 5). A transverse fracture extends about halfway through the nasals, so the specimen is composed of two parts. The premaxilla is fractured at the level of the anterior half of the nares, thus the anterior edge of the rostrum is missing. The left side of the posterior part of the cranium (made up of the left quadrate, jugal and quadratojugal) is also missing. The anterior part of the suture between maxillae and nasals is visible, as is the suture between nasals and premaxillae, showing clearly that the nasals do not enter the external nares (Fig. 5B). The prefrontal and lacrimal region is quite obscure because of the deformation and of the liquids used to preserve the specimen. Moreover, the lacrimals are incomplete. The supratemporal fenestrae are teardrop−shaped and long,

occupying almost half of the length of the neurocranial table. The neurocranium is only visible in dorsal view and has a very resinous aspect because of the varnish applied to it: most of the sutures are not visible, but the sutures between the frontal and the left postorbital, and between the frontal and the parietal, are appreciable (Fig. 5C). The right squamosal is fractured and slightly tilted. The posterior concavity of the squamosal is wide, with a clear tip laying on the paraoccipital process of the exoccipital.

Ventrally, the palatines are visible but in the area of the neurocranium the morphology is quite obscure and no character is distinguishable. The lower jaw shows a symphysis that extends approximatively to the 4th dentary alveolus.

MGP−PD 26814

This catalogue number refers to the lectotype of *Diplocynodon dalpiazi* (Fabiani, 1915). It is an almost complete skull, also with the lower jaws visible in ventral view, but is very deformed. In addition to the dorsoventral depression typical of all the Monteviale specimens, this skull has been exposed to remarkable lateral compression, so the left part of the skull, preserving the left external lower jaw, is well visible, whereas the right part is not distinguishable (Fig. S1D). It is one of the largest skulls, reaching at least 32 cm in length, but no suture is visible because the effect of the pyrite oxidation altered its fine morphology. The postorbital fenestra is triangular with a very short postorbital bar. The orbit is small: just under 4 cm in length and 3 cm in width. The skull is also incomplete at the level of the left lacrimal, but it might be possible to see part of the sutures between this bone and the adjacent nasal and jugal. The left squamosal is less deformed than the rest of the skull. The posterolateral process of the squamosal is uplifted respect to the skull table. There is probably a dislocation at the level of the suture between left quadrate and squamosal. The left articular and quadrate with the quadrate notch corresponding to the foramen aëreum are easily distinguished. The jugal is notably enlarged at the level of the postorbital bar.

Ventrally, the palate is strongly damaged and deformed. The left pterygoid, and partially the right one, are fully visible. The ectopterygoid is broken in undistinguishable from the pterygoid because of the action of the pyrite oxidation. The right mandible is almost complete, even if partially incomplete, in its posterior part, because there is a fracture that crosses the specimens at the level of the external mandibular fenestra. Here, we are able to count at least 14 (or 15) tooth positions. The left mandible has been tilted to the point that its medial surface is visible in ventral view—with the well−preserved articular element—and its external part is visible in dorsal view. The surangular−dentary contact is visible in the posterior part of the right mandible. The posterior−most part of the dentary is broken off, but the surangular shows a clear posterior tip ending anterior to the retroarticular process (character 72: 1).

MGP−PD 26815

This catalogue number refers to an incomplete anterior portion of a rostrum (Fig. S1E-F, 2C-D, 6E-F). Its bones are very thick, larger than those of the other specimens, so it probably belongs to an old, morphologically mature individual. The rostrum fragment preserves the lower jaw and the maxillary dentition on its ventral surface. The dentary symphysis extends to the 4th dentary alveolus. The 5th maxillary tooth is large, the 4th tooth is absent, but the alveolus seems slightly smaller than the 5th. The palatines are not recognizable since it is impossible to identify the sutures between palatine and maxillary elements, indicated by Franco et al. (1992, tav. III, 2).

MGP−PD 26816 – 26817

These two specimens are described together because they represent the cranium and lower jaw of the same individual. The cranium is separated in two parts by a fracture that passes through the orbits. The anterior part is nearly complete, whereas the posterior one is highly fragmented, with the jugal area of the skull missing on both sides. The nasals are short and therefore do not enter the external nares, as they stop at least two alveoli posterior to the posterior rim of the nares. Several

alveoli of the right maxilla are visible: at least 12 maxillary and 4 premaxillary teeth are preserved and visible. The premaxillary−maxillary suture ends in the notch corresponding to the 4th dentary tooth. The foramen incisivum is not very wide and it is far from the teeth. The skull table is crossed by a fracture at the level of the left supratemporal fenestra. The left squamosal is entirely missing, whereas the right one is broken off in the part that contacted the parietal. The left region is slightly more complete than the right one, as part of the quadrate is preserved in connection with the articular (and possibly the surangular), whereas part of the right quadrate is only preserved as a separate fragment, together with part of the quadratojugal. In this fragment, the dorsal notch of the quadrate for the foramen aëreum (character 179: 1) is visible. As far as the attachment scar for the posterior mandibular adductor muscle on the ventral surface of the quadrate is concerned, it can be reconstructed to have been present as a modest crest (character 178: 0), through the whole crest is not present, but only its posteriormost part.

The lower jaw is highly deformed and incomplete so that the detailed morphology cannot be assessed. It was also broken in two points, but was subsequently reunited. Even if the dental alveoli are not visible, it can be stated that the two fractures passed more or less at the level of the 5th right alveolus and of the 7th left one.

MGP−PD 26843

MGP−PD 26843 is the lectotype of *Asiatosuchus monsvialensis* (Fabiani, 1914). This specimen is an almost complete skull, dorsoventrally depressed (Fig. S1A-B, 6A-C). The lateral deformation seems to be negligible. Surprisingly, the anterior end of the nasals has been figured by Franco and Piccoli (1993: pl. I,1) as reaching the external nares, whereas they are actually at least 12 mm far from each other. The relationship among nasals, prefrontals, and frontal is consistent with the specimens described above. The sutures of the lacrimals are not clearly visible. The jugal is dorsoventrally enlarged at the level of the postorbital bar, even if not as much as in the specimen

26814: in this case, it is slender. The jugal and the quadratojugal are slightly disarticulated at the level of the evident suture, whereas the suture between quadrajugal and quadrate is only perceivable. In ventral view, the surface of the skull is significantly altered and, even if some areas are more discernible (e.g. the posterior part of the palatines showing reciprocal contact), the general morphology of the palate cannot be assessed.

MGP−PD 26844

This is a quite complete skull aside from the missing left postorbital region (Fig. 2A-B). It is very compressed dorsoventrally and it is one of the skulls most treated with varnish, to the point that, especially in dorsal view, almost nothing can be said about its morphology and sutures. Ventrally, the posterior part of each palatal fenestra is visible. The dental pattern can be reconstructed in the left maxilla, which bears at least 13 alveoli, with the 4^{th} and the 5^{th} alveolus confluent but with the 4^{th} smaller than the 5^{th}.

MGP−PD 26845

This skull is affected by severe deformation. The anterior part of this skull is broken off and the cranium is significantly deformed, with a marked lateral deformation, which obliterates most of the left part of it (Fig. S1C). The right portion of the skull is represented by the jugal with an evident infratemporal fenestra and by part of the parietal table, making up the supratemporal fenestra. The anteromedial edge of the orbits is elevated in a crest, which, together with the frontal step forms the spectacle. Ventrally, the deformed mandible occupies most of the space, and the palatal structure cannot be reconstructed.

MGP−PD 26846

MGP−PD 26846 is a skull highly fractured and intensively treated with varnish. The anterior portion of the rostrum is missing, and so are both lateral sides. Because of the extensive painting which covers the bones, no characters are scorable on this specimen.

MGP−PD 26850

This catalogue number refers to the anterior part of a skull broken at the level of the anterior edge of the orbits. The external nares are not bisected by the nasals, which are excluded by the nares (character 82: 2). It is one of the skulls where the sutures are the clearest: all the sutures of the nasals and the sutures between prefrontal and lacrimals are easily distinguished (Fig. 4A-B). The lacrimal makes broad contact with the nasal and there is no posterior process of the maxilla (character 127: 0). The prefrontal is uplifted in its posterior part, forming part of the bony eyelid, typical of alligatoroids.

Ventrally, the dentary symphysis extends, as in the other specimens, to the 4th dentary tooth.

MGP−PD 26858

This catalogue number refers to a skull affected by significant deformation, in which the anterior right part of the rostrum is missing (Fig. 4C-D). The deformation is clear at the level of the orbits, which look very different in shape from one another; the left is more triangular than the right one. The postorbital bar is short and hidden by the displaced surrounding bones (as in MGP−PD 26814). The neurocranium is relatively well preserved, showing the typical wide supratemporal fenestrae. The sutures between the postorbitals and the prefrontal are clearly visible; in particular, in the left area these two bones are separated at the level of the suture. The contact between the left jugal and quadratojugal is visible, but the infratemporal fenestra is dorsoventrally depressed and thus it is not possible to evaluate if the suture between them lies ventrally, dorsally, or corresponding to the

posterior angle of the fenestra (character 140). In lateral view, cervical vertebrae are evidently deformed and mostly covered by disarticulated osteoderms. Ventrally, the palatal region is partially covered by the highly deformed left mandible, but there are some characters worth noting. In fact, the posteromedial part of each suborbital fenestra is well preserved (Fig. S1D) and it can be discerned that the palatine−pterygoid suture is far from the posterior corner of the suborbital fenestra (character 117: 1) and that the lateral edges of the palatines are parallel posteriorly, without producing a shelf (character 119: 0). Moreover, even if the choana is not visible, the anteriormost part of the pterygoid contacting the palatine is intact, meaning that the choana is entirely surrounded by pterygoids (character 120: 1; Fig. S1D). The pterygoids are broken next to the base on both sides. Posterior to the cranium, there is also the proximal part of a humerus, with two skeletal elements. For the description of this specimen's hindlimb portion, see below (postcranium section).

Variably isolated skull elements

Besides the numbered specimens described in this section, there are seven fragments of mandibles and maxillae and more than 40 disarticulated teeth that do not have any catalogue number. Because of their highly fragmentary nature, the description is omitted but they have been examined, and, as their morphology is congruent with the described, numbered specimens, they have not been listed here.

MGP−PD 8648

MGP−PD 8648 is a right maxilla in occlusion with the lower jaw. The maxilla is fractured in two points, in those points in which the maxilla is notched, and therefore weaker than in the other areas: after the 4^{th} mandibular tooth and after the 7^{th} maxillary tooth (Fig. 8). The dentition pattern can be evaluated better than in all the other specimens. The 4^{th} mandibular tooth is inserted in the typical premaxillary−maxillary notch. The premaxillary teeth are five, and because the only ontogenetic change can be a reduction in number (from five to four), character 87 (number of premaxillary

teeth) is scored as 0 (5 premaxillary teeth). There are at least 12 maxillary teeth. The 4th maxillary tooth projects from the alveolus, seeming larger than the 5th, but actually, the 5th alveolus is clearly larger than the 4th.

MGP−PD 26819

This catalogue number refers to three very deformed fragments of a right maxilla and lower jaw in occlusion. One of the fragments preserves part of the mandibular symphysis, whose extension cannot be reconstructed because of the high level of deformation of the specimen. The medial internal surface is badly preserved and the anterior extension of the splenial is not visible. A few alveoli are still preserved but due to the incompleteness of the tooth row it is not possible to add further details.

MGP−PD 26835

MGP−PD 26835 is the posterior, left portion of a skull, with the posterior part of the lower jaw still in anatomical position. Dorsally, next to the teardrop−like supratemporal fenestra, the suture between the postorbital and the squamosal can be discerned. The suture between quadrate and quadratojugal is visible at least in the area near the articular process. Ventrally, the choana is central in the pterygoid. The notch of the quadrate is particularly evident.

MGP−PD 26837

This catalogue number refers to a portion of maxilla and lower jaw pasted together in a non−anatomical position. The interpretation of the structures is thus impossible.

MGP−PD 26838

This catalogue number refers to two fragments of left and right mandible from a single specimen. On the left mandible it is visible the part of the suture between splenial and dentary corresponding to an area far from the symphysis, and thus unfortunately no character can be scored.

MGP−PD 26839

MGP−PD 26839 refers to 40 disarticulated teeth. Their shape is the classic conical shape, slightly curved, with evident mesiodistal carinae. Their labial and lingual surfaces are smooth (although a hint of longitudinal ridges is present). In all teeth, the limit between the crown and the root is marked by a faint constriction. The crown can display numerous transverse lines representing growth marks.

MGP−PD 26842

This catalogue number refers to a fragment of mandible that still hosts three teeth in the alveoli. The specimen is covered by varnish, obscuring its morphology.

MGP−PD 26957

This catalogue number refers to a fragment of mandible (possibly the right one) with a clear portion of splenial, but unfortunately without any visible suture. There are three teeth, of which just one is complete. Moreover, an empty alveolus is present.

MGP−PD 26859

This specimen is a slab with a portion of the vertebral column and with the posterior part of a left mandible with the articular region of the skull. The quadrate is visible with a small foramen aëreum

(character 176: 0) on its dorsal surface (character 175: 1). The foramen aëreum is not perceivable on the retroarticular process because of preservational reasons.

MGP−PD 26862

This catalogue number refers to a portion of undeformed left rostrum. Part of the left external naris is visible, and the anterior and lateral margins of it are developed into a marked crest (Fig. S2A-B-C). No teeth are visible. In the ventral part of the specimen there are several disarticulated osteoderms in various orientations.

MGP−PD 31998

This catalogue number refers to various fragments of unidentified maxillary parts and a portion of right pterygoid, particularly ruined. The ectopterygoid−pterygoid flexure is not present because the suture is rather straight (character 125: 0) and the ectopterygoid clearly does not extend to the posterior tip of the lateral pterygoid flange (character 126: 1; Fig. S2D, 6D).

Postcranium

As for the parts of the cranium, there are several unnumbered specimens that have been examined and which are not reported in detail because they are mostly unidentified limb fragments, disarticulated osteoderms, or vertebrae. These specimens include five slabs with poorly prepared and damaged portions of the vertebral column, five isolated vertebrae, seven slabs with fragmentary and disarticulated limbs, several ribs and osteoderms.

MGP−PD 27999 and 26854

MGP−PD 27999 is a big slab containing the lumbar portion of an individual (Fig. S3A-C, Fig. 7D-F). The vertebral column is exposed in ventral view, composed by 8 vertebrae, of which 6 are still articulated. There is also a part of the disarticulated pelvic girdle. The single bones are difficult to

interpret: the smaller bone perhaps represents the proximal part of the ischium with the distal part broken and moved forward, whereas the larger bone (shown in Fig. S3B) could be the pubis. There are also some portions of the ilium which are highly fragmented and disarticulated. Next to the pelvic girdle there are some thin long bones that can be interpreted as remains of the gastral apparatus. On the opposite part of the slab there are some fragments of ribs. The dorsal osteoderms, with the typical midline keel, are only visible in a single line of articulation and thus the number of lines of dorsal osteoderms cannot be reconstructed. The ventral osteoderms are articulated and clearly bipartite (Fig. S3C).

MGP−PD 26854 is complementary to MGP−PD 27999, representing the prosecution of the left side of this individual. In this slab, the line of keeled dorsal osteoderms continues and next to it there is a disarticulated zeugopodium, probably composed of the left radius and ulna, and a broken distal part of the humerus (Fig. S3A). The vertebral elements are represented just by the vertebral body.

MGP−PD 26818

This slab hosts at least one vertebra, some dorsal keeled osteoderms, and two partial disarticulated limbs including a humerus.

MGP−PD 26820

A fragmented, very altered specimen, which contains a lot of disarticulated osteoderms that obscure most of the underlying bones. The preserved long bones cannot be identified.

MGP−PD 26821

MGP−PD 26821 is a slab with a portion of vertebral column, some disarticulated ribs or gastralia, and numerous osteoderms (Fig. S3E). The vertebrae are at least five, in ventral view, and without

hypapophysis. Most of the osteoderms are visible in ventral view. Only one of them is surely a dorsal vertebra, as it presents the typical keel.

MGP−PD 26822

This slab shows some disarticulated and fragmented bones of the pelvic girdle. Three girdle bones are recognizable: one ischium, with a concavity on the proximal part, and two pubes. Moreover, there is a chevron and two vertebrae, which could be the two sacral elements. The most complete of these vertebrae is preserved in ventral view and shows a vertebral body and a transverse process, whereas the other one is represented by a small fragment.

MGP−PD 28623

This catalogue number refers to a single slab fragmented in three portions, containing part of a vertebral column, a number of disconnected ribs, and several osteoderms (Fig. S3D). The vertebral column is composed of seven articulated vertebrae. On four vertebrae there are the hypapophyses, which are not present in the other three, which means that this part of the column is composed of dorsal vertebrae. In the right part of the column there are two dorsal osteoderms, whereas in the left part a lot of ventral osteoderms are present.

MGP−PD 26824

This catalogue number refers to a slab with fragmented, disarticulated bones, some of which unidentifiable, and osteoderms (Fig. S2E). Some of these bones are of the pelvic girdle (possibly an ischium and a pubis, but it is very difficult to say, because of the bad preservation of the specimen), and the proximal epiphysis of the femur.

MGP−PD 26825 – 26830

These two catalogue numbers refer to a fragmented slab (Fig. S4A). MGP−PD 26830 is represented by an incomplete vertebral body in ventral view, with the right transverse process, part of a limb (probably part of the zeugopodium and of the autopodium), and an isolated, broken osteoderm. The vertebral body of MGP−PD 26830 is broken and fits perfectly the broken portion of a vertebra present in MGP−PD 26825. This vertebra is only slightly dislocated with respect to other two vertebrae present on the slab MGP−PD 26825. These two vertebrae, in ventral view, are procoelous, with both the transverse processes preserved, approximately as long as the vertebral body. Next to these vertebrae there is a chevron, which, together with the length of the transverse processes, suggests that they are caudal vertebrae. On this slab, there is also another portion of a vertebra, some disarticulated ribs, and a chevron.

MGP−PD 26826

This altered slab contains several osteoderms, some incomplete vertebrae, and disarticulated fragments of gastralia or ribs. The osteoderms cover most of the underlying portion of the bones, which are thus unidentified.

MGP−PD 26827

This very altered slab contains some damaged vertebrae and some disarticulated bones including osteoderms.

MGP−PD 26828

This small, very altered slab contains several disarticulated ventral and dorsal osteoderms, together with a long, unidentified bone.

MGP−PD 26829

This slab hosts a broken, proximal portion of the zeugopodium, probably a radius and ulna. The articular surface is not visible. The two bones partially overly one another.

MGP−PD 26831, 26832, 26833 and 26834

These catalogue numbers refer to different fragments belonging to the same individual. The fragments are small, and very altered because of pyrite. There are some ribs and several osteoderms, which obscure the other bones.

MGP−PD 26836

This catalogue number refers to a fragment of an elongated, unidentified bone.

MGP−PD 26840

Slab with a portion of a posterior limb and of the caudal vertebral column (Fig. S4E). The posterior limb is composed of a complete autopodium and zeugopodium, whereas the femur is broken at the level of the distal epiphysis. In the vertebral column, there are six vertebrae with the relative lateral osteoderms.

MGP−PD 26841

This catalogue number refers to a slab with an almost complete posterior limb with few isolated osteoderms (Fig. S4D). The femur and the zeugopodium are complete. The femur is slightly longer than the zeugopodium and curved in both its proximal and distal part. The autopodium is partially preserved.

MGP−PD 26847

MGP−PD 26847 is a slab with several articulated dorsal osteoderms. The osteoderms have the typical keel and are disposed in four parallel lines (Fig. S4B). Lateral to the osteoderms there is a wide and short bone that is probably a coracoid.

MGP−PD 26848

This catalogue number refers to a large slab with many disarticulated osteoderms, of which one is surely dorsal. The slab is ruined because of pyrite oxidation, and very little can be said about it. One unidentified bone of the scapular girdle is also present.

MGP−PD 26849

This slab hosts articulated.ventral and dorsal osteoderms. Moreover, there are at least ten vertebrae, of which 4 only slightly disarticulated. A portion of the anterior left limb is visible, with the humerus fractured in the proximal part, the zeugopodium and some disarticulated phalanges. The pelvic area is very altered and there are several fractured bones, including two disarticulated femora.

MGP−PD 26851

This slab preserves a fragmented anterior limb. The autopodium and the articulation between humerus and radius and ulna are missing. The proximal part of the humerus is broken and the characters of phylogenetic relevance are not visible.

MGP−PD 26852 and 26853

These two catalogue numbers refer to a single slab that contains several poorly preserved osteoderms (Fig. S4C). Among them, there are some unidentified bones and a limb, possibly

anterior, in which the articulation between the stylopodium and the zeugopodium is clearly visible. The autopodium is not visible, as it is covered by the osteoderms and partially broken off in its distal part.

MGP−PD 26855

This catalogue number refers to a very altered slab with some disarticulated osteoderms, four fragments of disarticulated ribs and a portion of a scapular girdle (Fig. S5A). The two flat bones are a scapula and a coracoid, still in articulation, showing the glenoid surface in which the humerus inserted. The humerus itself is missing (Fig. S5B).

MGP−PD 26856

This catalogue number refers to an axis (Fig. S5C) pasted in non−anatomical position with several osteoderms (Fig. S5C,D). The axis is at least five centimetres long. The anterior crest is assumed to be horizontal, even if it is possible that it is broken. Next to the posterior neural margin it has been pasted an extraneous bone. The posterior part of the vertebral body was broken off and the resulting pieces were glued together in non−anatomical position. The left lateral portion of the neural arch is medially compressed. The ventral region is damaged and the hypapophysis is not visible.

MGP−PD 26858 (continuation)

Posterior to the cranium of this specimen described in the skull section, in the ventral part of the specimen there is also the proximal portion of a humerus, whose deltopectoral crest is partially preserved. The concave proximal edge of the deltopectoral crest is not evident, but it emerges abruptly from the proximal end of the humerus (character 27: 1). There is also a flat bone, probably a coracoid, and another unidentified skeletal element.

MGP−PD 31997

This catalogue number refers to a fragmentary first sacral vertebra (Fig. S5E). The neural spine is missing. Part of the left transverse process is present, but it is deformed, with a sliding plane between the capitulum and the tuberculum, so that it is not possible to state if the capitulum projects

anteriorly of tuberculum or if they are nearly in the same plane (character 22). It seems that the capitulum projects anteriorly of the tuberculum, but it seems to be a taphonomic effect. The right transverse process, conversely, is broken off.

NMB−Bc.6 (Basel)

NMB−Bc.6 is represented by a complete, depressed skull and several postcranial fragments of a single individual (Fig. 1). All the parts of the specimen were extracted from the lignite slab that formerly hosted them, 3D prepared and then treated against pyrite disease. In order to maintain them in the original spatial association, the remains were laid down on a resin support that mimics the original lignite slab. Besides the large individual to which most of the fragments probably belong, there are some fragments surely representing another, much smaller, individual: part of a quadrate, some disarticulated bones, comprehending a scapula and a small vertebra (A in Fig. 1). Moreover, in the posterior part of the large individual, there is a fragment with small teeth, most likely belonging to another small individual (therefore a third one), as they are the typical conical crocodile teeth (B in Fig. 1). Minor shearing affects the skull, whose rostrum is cut by a transverse fracture. In dorsal view, the suture pattern is difficult to discern, but can be assessed in some portions of the skull (Fig. 3). The skull seems to be quite asymmetrical, probably due to taphonomic deformation. In ventral view, the mandibular rami are visible (Fig. S6), but the palatal structure is only slightly perceivable, as the ventral surface is much worse preserved than the dorsal one.

Skull – The right side of the cranium is broken at the level of the contact between lacrimal and nasal. The premaxilla bears short dorsal processes, not extending beyond the third maxillary alveolus (character 90:0), visible even considering the fracture that crosses this area.

On the left side, the lacrimal tapers relatively far anteriorly at about the level of the sixth maxillary alveolus and therefore extensively contacts the posterolateral margin of the nasal. Whether or not a process of the maxilla extends between the lacrimal and the nasal cannot be stated, because the suture is not evident enough in that area. The prefrontal does not extend as far as the lacrimal, but is quite elongate. The frontal separates the posterior tip of the two nasals.

Given the quite elongate rostrum, the orbital region does not extend into the anterior half of the skull and is characterized by a narrow interorbital width and by small orbits. The anterior projection of the frontal is narrow. The interorbital region is marked by a well-delineated preorbital ridge passing through the frontal and following the anteromedial margin of the orbits on the prefrontal and lacrimal. The anterior−most margin of the orbits is formed by the lacrimal and is notched.

The compression of the skull table has mostly a vertical component, but with a slight anterolateral direction, so that the exoccipital faces dorsally. The supratemporal fenestrae are circular. As in the Padua specimens, the frontoparietal suture extends to the supratemporal fenestrae, preventing the postorbital from contacting the parietal on the skull table. The space between the supratemporal fenestrae is wide. The supraoccipital clearly participates in the dorsal surface of the skull table, but does not prevent the parietal from reaching the posterior margin of the table. The squamosal prongs seem to project posteriorly, but this is actually due to the forward compression of the skull table, which permits observation of the exoccipital surface and the squamosal prongs descending along this bone. Actually, the squamosal prongs are short and do not project far posteriorly nor laterally. On the medial wall of the right supratemporal fenestra, two foramina are clearly visible. The suture organisation around the lower temporal fenestra is best seen on the left side. This temporal fenestra seems very narrow and elongate but this may be an artefact of compression. The quadratojugal forms the posterior corner of this fenestra. The quadratojugal spine cannot be observed, and the postorbital bar is barely visible. The quadrate branches do not project extensively beyond the level of the skull table. The small medial quadrate hemicondyle bears the notch for the foramen aëreum on its dorsal surface, as evidenced from the right quadrate. The exoccipital is largely exposed, even if deformed.

The mandible is deformed and fractured in various locations, to the point that no sutures can be identified. The right articular is visible in dorsal view and reveals the presence of the foramen aëreum, which is laterally shifted, positioned in line with the corresponding foramen of the

quadrate, and set in from the margin of the retroarticular process (character 70:1). The retroarticular process is deeply concave and its tip projects posterodorsally. The right external mandibular fenestra is not particularly wide, thus the foramen intermandibularis caudalis, even if not directly identified, can be reconstructed to have not been visible through the fenestra (character 63:1).

The basioccipital is visible (Fig. S6C), bearing a prominent medial crest, but because of the deformation it is not possible to identify its orientation (character 168).

Dentition and Occlusion—The maxilla has a pair of caniniform teeth on the left side corresponding to the fourth and fifth teeth. There is an overbite of the premaxillary and maxillary bones over the dentary. Only one large dentary tooth is visible at the level of the left premaxillary−maxillary notch.

Postcranial Skeleton—Limited information can be gained from the postcranial elements. They were partly dissociated before burial of the animals as testified by the incompleteness of the Basel specimen, which lacks the posterior trunk region, the limbs, and a big portion of the cervical area (Fig. 1). The ribs are in some cases present, but disarticulated and broken.

Posterior to the exoccipital of the skull, the first three – and part of the fourth – cervical vertebrae are still in articulation, even if rotated and visible in left lateral view (Fig. 3C). The part of the atlas which is most visible is the right neural arch, while the left neural arch and the intercentrum are just perceivable by some evident parts surrounding the occipital condyle. The axis has a prominent neural spine, which is broken in its apical part and therefore the presence of a crest is equivocal (character 12). The hypapophysis of the third vertebra is not visible, but there is a break between its parapophysis and the parapophysis of the axis that could be the evidence of a structure, interpretable as the lost hypapophysis (character 18:0).

The ribs are not visible in the dorsal part of the specimen. The situation is different in its ventral part, where the neural spine of the axis is covered by two (or three: see Fig. S6C) ribs. Based

on its shape, one of them is reconstructed to be one of the atlantal ribs – whose bad preservation prevents the identification of diagnostic characters – and the other one, based on its shape and on its position, one of the axis' ribs, which seems to be still in anatomical connection with the odontoid process of the axis. Another rib is present under the left part of the skull, posteriorly to the left ectopterygoid, and partially contacting it.

In the preserved trunk portion, neural arches are here visible and indicate the midline of the trunk. There are at least four rows of dorsal keeled osteoderms. Among these, in the right part of the trunk, one row composed of three rectangular osteoderms seems to be complete, because there is a small osteoderm which is visible in both ventral and dorsal view, in the same position it should have had during the life of the individual. This osteoderm is likely a lateral osteoderm. For this reason, the osteoderms are supposed to have been three per side (Fig. 7A-B; character 40:1). The anterior margin of at least one osteoderm, the only one whose anterior part is not covered by other osteoderms, shows an anterior process (character 43:0; Fig. 7C). Each series of osteoderms overlaps the next series located posterior to it. On the contrary, the ventral osteoderms do not overlap each other.

A single sacral vertebra is present as an isolated fragment between the skull region and the thoracic region. Because of its position it seems unlikely that this vertebra belongs to the same large individual, and it seems more probable that it belongs to another, maybe smaller, individual. The sacral vertebra is the first one because the anterior part of its centrum, recognizable because of the position of the transverse process, is concave. Thanks to this information, all the vertebrae can be considered as procelous (character 21:1).

The scapula, most likely belonging to the same small individual of the vertebra, is the only limb girdle bone clearly identified, and its blade flares dorsally (character 23:0).

MLR – no number

The La Rochelle specimen is located on a lignite slab, somehow similar to the Basel one, but it has not been prepared in 3D, being still embedded in the original matrix. It bears a skull and disarticulated and fragmented portion of the postcranial skeleton.

Skull – The skull is visible in dorsal view and is dorsoventrally compressed. The La Rochelle skull is more affected by shearing in the right anterolateral direction than the Basel one, obscuring the right mandibular ramus. The suture pattern is difficult to discern, but can be assessed in some portions of the skull. The skull is relatively broad, presenting wide premaxillae, a curved maxillary contour at the level of the largest teeth and diminutive orbits. However, the rostrum is quite elongate, the interorbital space is relatively narrow and the skull table is not expanded laterally and does not project posteriorly.

The anterior region of the rostrum is massive with an almost straight anterior margin of the premaxillae. The external nares are nearly rectangular, being slightly longer than wide. The anterior region of the rim of the nares is flat and continuous with the external margin of the bone. The nasals are excluded from the posterior margin of the nares by a thick expansion of the premaxilla at the level of the premaxillary−maxillary notch. The antorbital region is obscured, and suture organization is uncertain. The skull table has been mediolaterally deformed, thus affecting the shape of the supratemporal fenestra. The frontoparietal suture penetrates between the supratemporal fenestrae, preventing the postorbital from contacting the parietal on the skull table. The squamosal prongs are short and do not project far posteriorly nor laterally. The suture organisation around the lower temporal fenestra is best seen on the left side. The lower temporal fenestra seems very narrow and elongate, but this may be an artefact of compression. The quadratojugal forms the posterior corner of this fenestra. The postorbital bar is partially preserved. The small medial quadrate

hemicondyle bears the notch for the foramen aëreum on its dorsal surface, as evidenced from the right quadrate.

The position of various sutures in the mandible is difficult to assess due to preservation. A long crack runs in the posterior portion of the mandible, passing through the external mandibular fenestra. A suture departs from the posterior level of the fenestra and continues to the tip of the retroarticular process. This suture separates the surangular from the angular. The articular is visible in dorsal view and reveals the presence of the foramen aëreum, which is laterally shifted and positioned in line with the corresponding foramen of the quadrate. The retroarticular process is deeply concave and its tip projects posterodorsally.

Dentition and occlusion—The fourth maxillary tooth is smaller than the fifth and be in the process of being replaced. Part of the anterior maxillary tooth row is visible up to the sixth tooth, which is considerably smaller than the fifth one. Only one large dentary tooth is visible at the level of the left premaxillary−maxillary notch.

Postcranial skeleton—Limited information can be gained from the postcranial elements. Only the left forelimb is still partially articulated and most of the dorsal osteoderms and the trunk vertebrae are missing. The posterior region is incomplete with disarticulated hindlimbs including two femora, partially articulated tarsal bones and some caudal vertebrae in connection.

Below we present a photographic atlas of most of the material from Monteviale housed in MGP.

NHM-UK 2789

The London specimen is a 50x50cm slab on which is a badly preserved part of a small individual, most likely a juvenile. It is visible in dorsal view, with the dorsal armor composed of six rows of keeled osteoderms. There is only one osteoderm with the anterior, smooth part is visible, but it is broken so that the interior process is not recognizable. There are also the whole hindlimbs, except

for part of the autopodii, and part of the left forelimb, in particular the zeugopodium and the stylopodium.

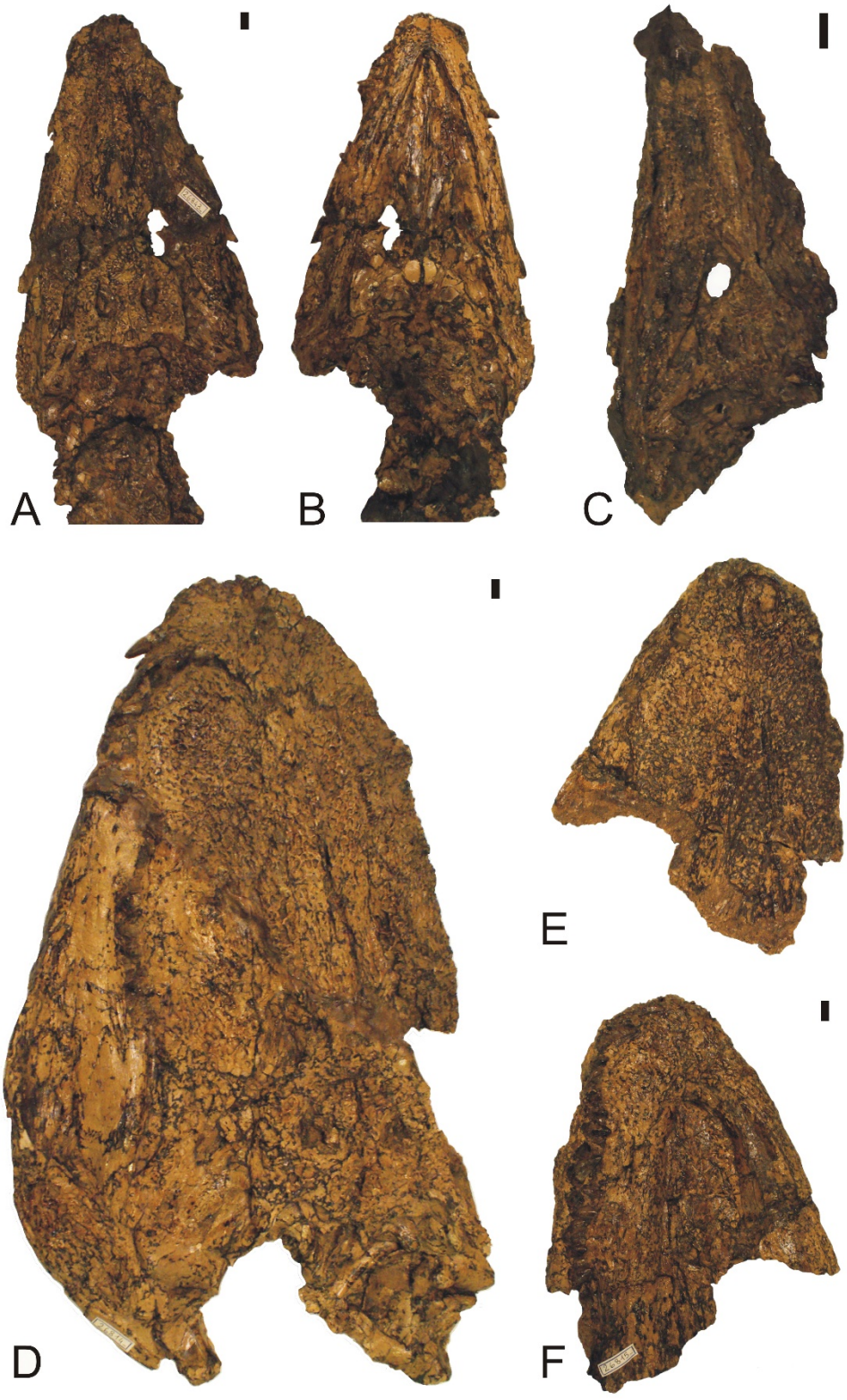

Figure S1. Selection of Padua skulls: MGP−PD 26843 in dorsal (A) and ventral (B) view, 26845 in dorsal view (C), 26814 in dorsal view (D), 26815 in dorsal (E) and ventral (F) view. Scale bars 1 cm: in the right, low corner in A, and in the right, high corner in D and E.

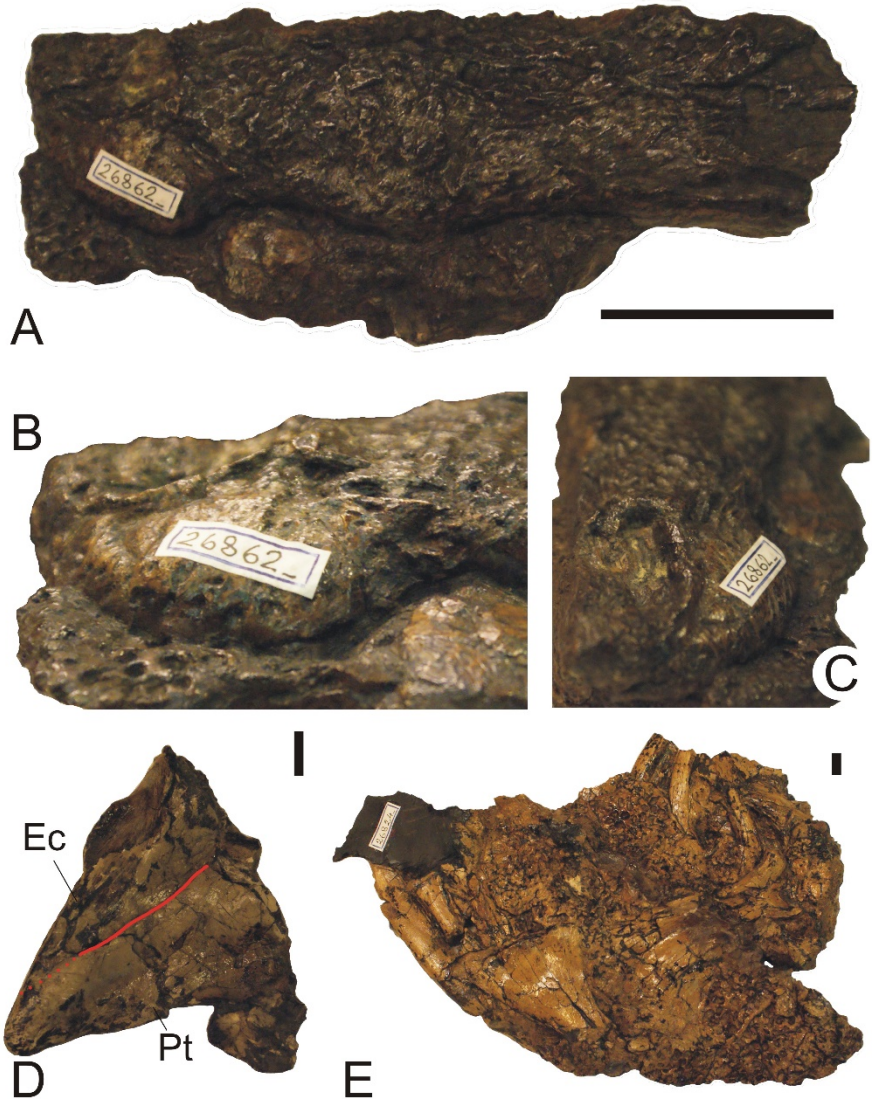

Figure S2. Left part of a rostrum (MGP−PD 26862) in lateral (A, B) and frontal (C) view. D) right pterygoid wing in ventral view (MGP−PD 31998) showing the contact between pterygoid (Pt) and ectopterygoid (Ec). E) unidentified postcranial element (MGP−PD: 26824). Scale bars 1 cm.

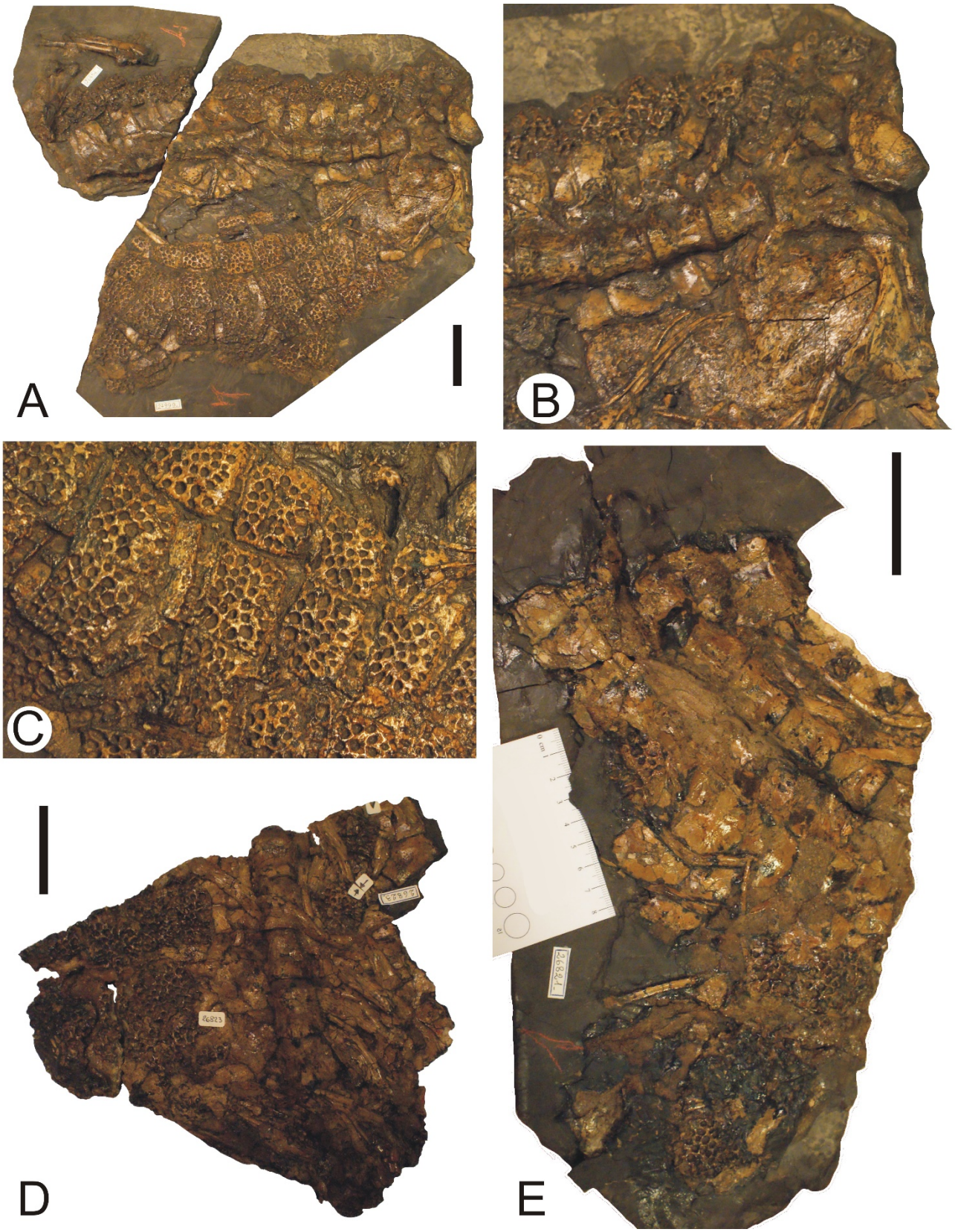

Figure S3. Postcranial elements from Padua. A) part of a dorsal vertebral column (MGP−PD 27999 and 26854). B,C) details of A: ischium (B) and ventral, bipartite osteoderms (C). D) part of a

vertebral column in ventral view (MGP−PD 26823). E) articulated vertebrae with osteoderms in ventral view (MGP−PD 26821). Scale bar 5 cm.

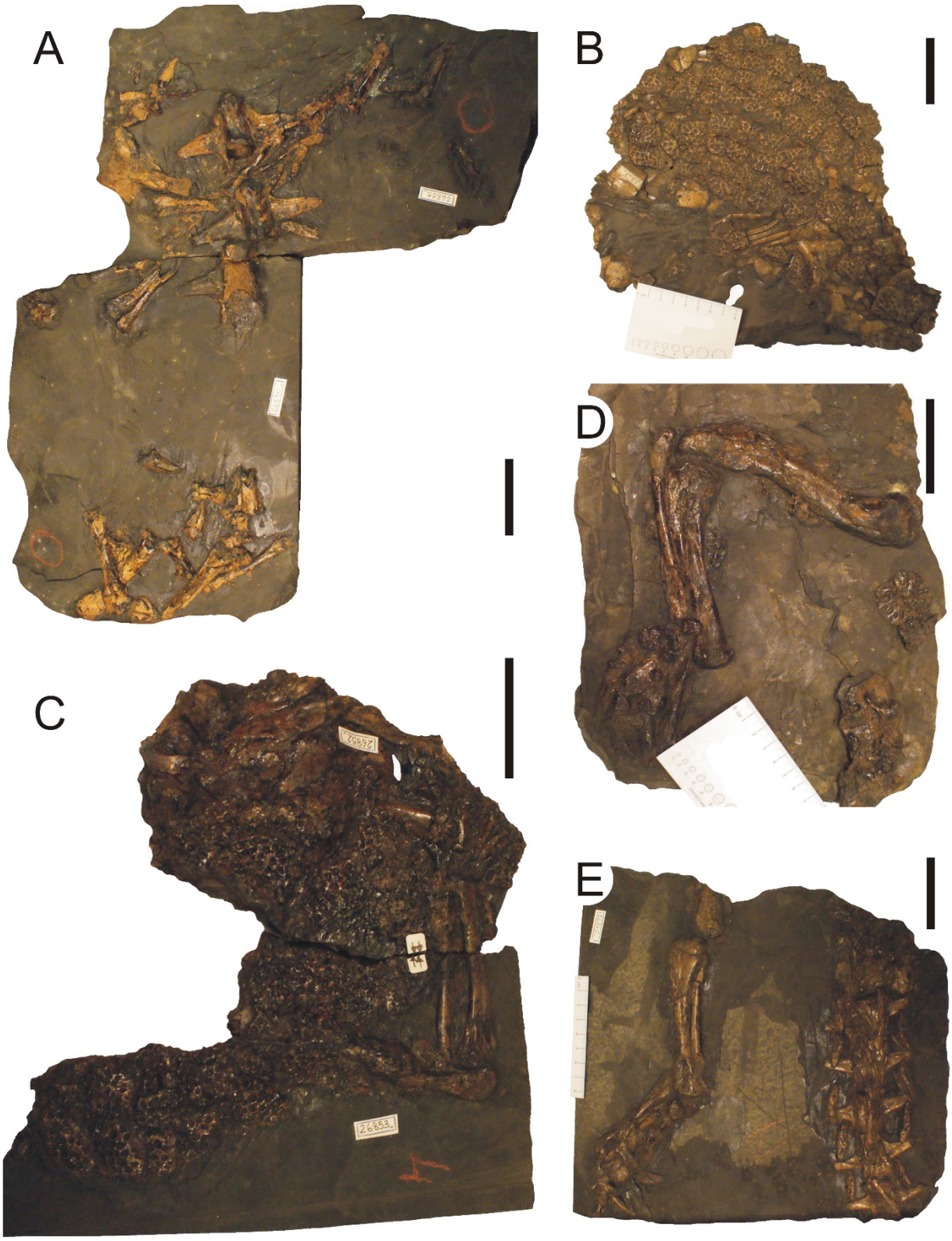

Fig. S4. Postcranial elements from Padua. A) disarticulated vertebrae (MGP−PD 26825 and 26830). B) dorsal osteoderms (MGP−PD 26847). C) limb element covered by osteoderms (MGP−PD 26852 and 26853). D) almost complete limb element (MGP-PD 26841). E) caudal vertebrae and distal part of a posterior limb (MGP−PD 26840). Scale bar 5 cm.

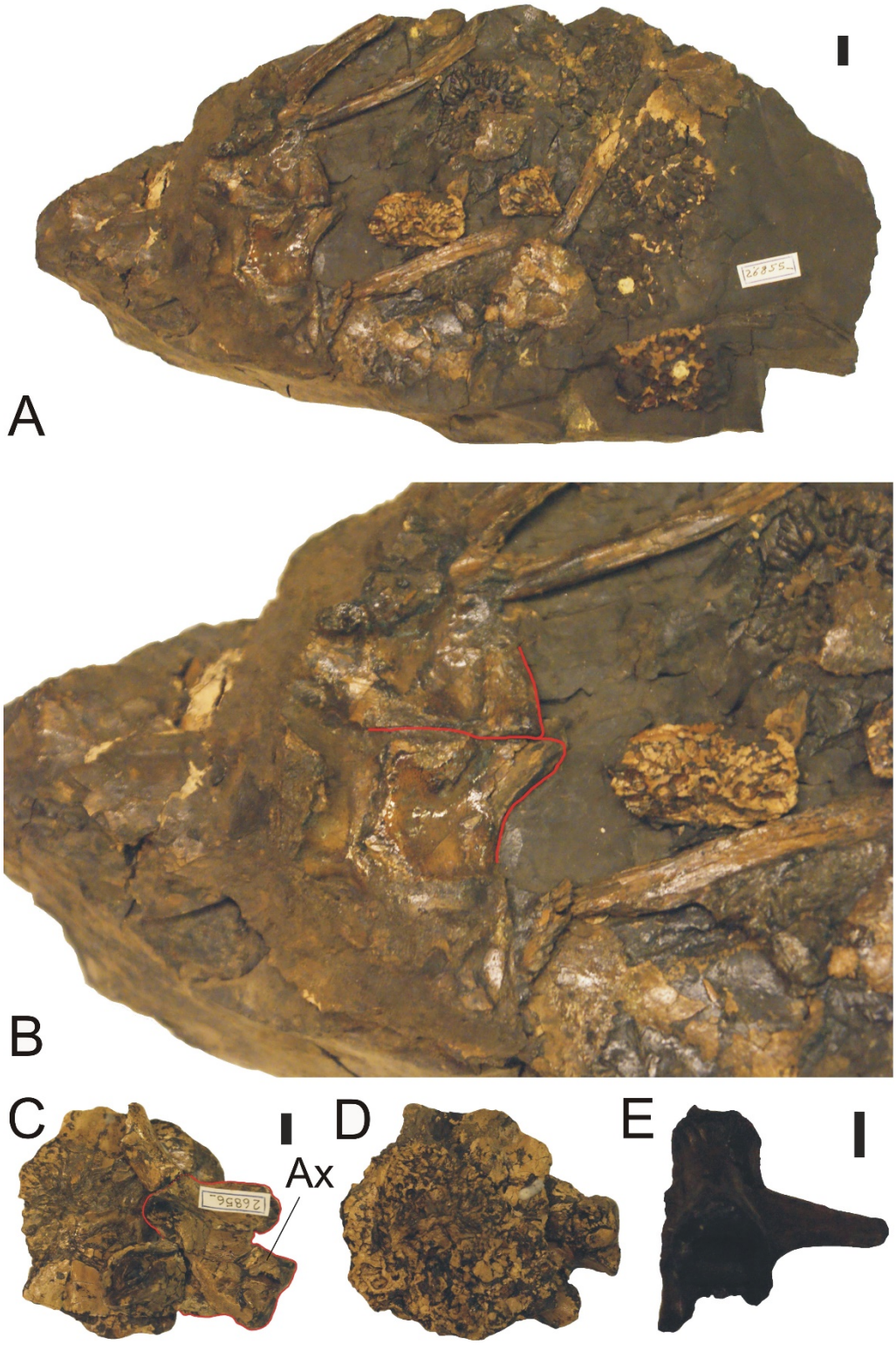

Figure S5. Postcranial elements from Padua. A) scapular girdle with ribs (MGP−PD 26855). B) interpretative drawing of A, showing the contact between scapula and coracoid. C,D) block of pasted osteoderms (MGP−PD 26856) containing an axis (Ax). E) first sacral vertebra (MGP−PD 31997). Scale bar 1 cm.

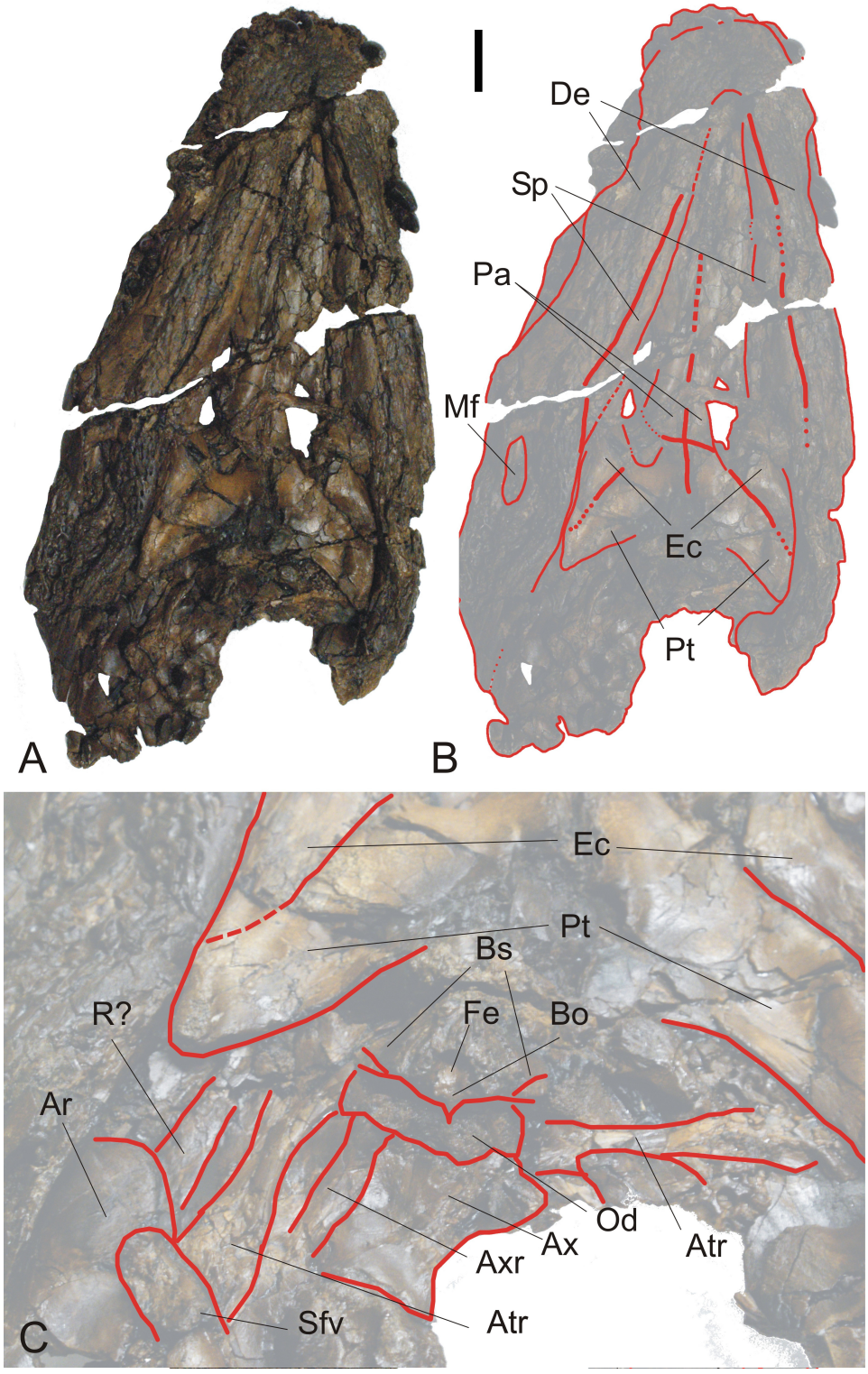

Figure S6. NMB−Bc.6 skull in ventral view. Scale bar 5 cm. Ar: articular, Atr: atlantal rib, Ax: axis, Axr: axis rib, Bo: basioccipital, Bs: basisphenoid, De: dental, Ec: ectopterygoid, Fe: Eustachian foramen, Od: odontoid process, Pa: palatine, Pt: pterygoid, R: rib, Sfv: spine of the fourth vertebra, Sp: splenial.

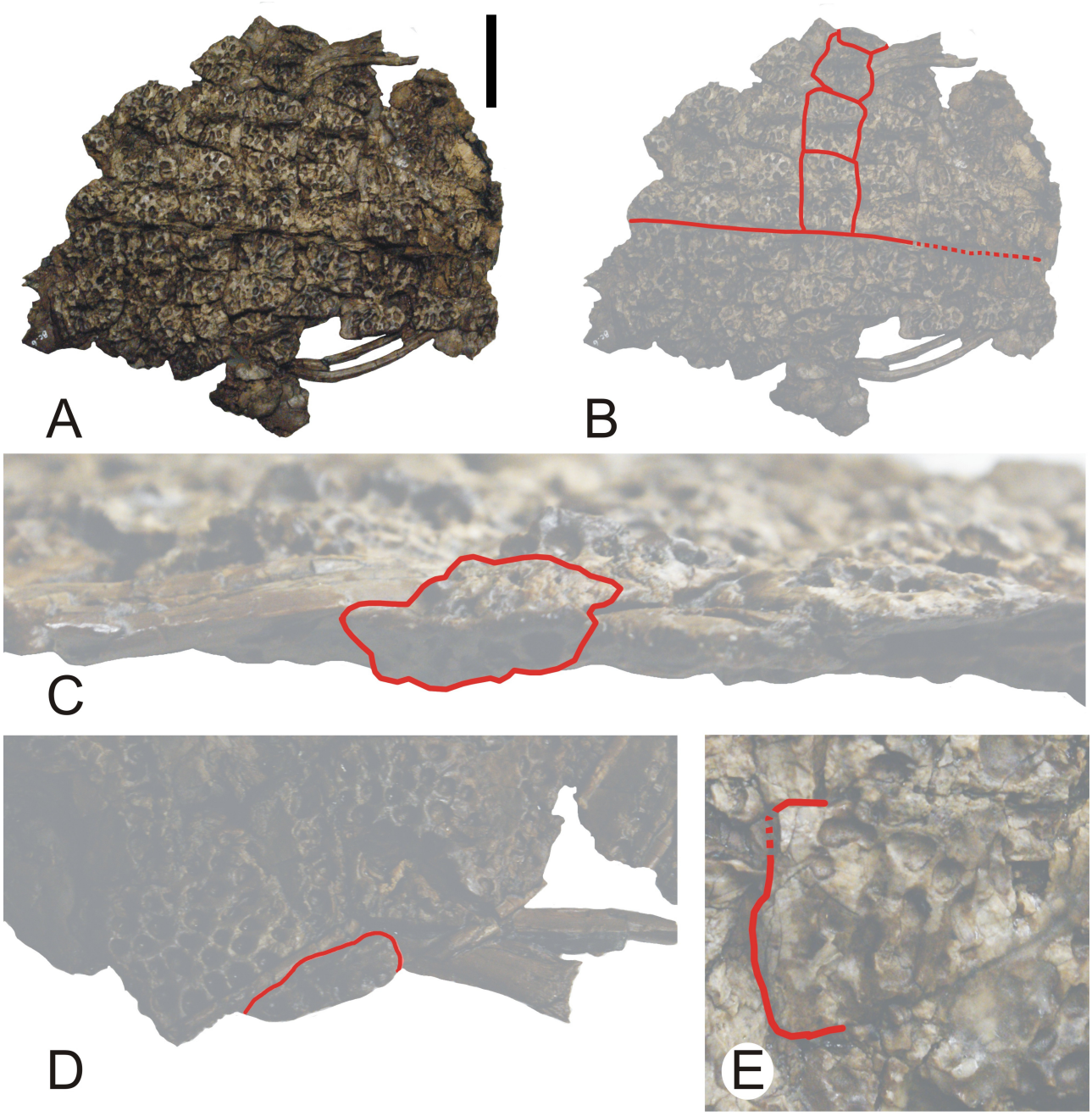

Figure S7. Dorsal (A) and ventral (D) armour of NMB−Bc.6. Lateral osteoderm in lateral (C) and ventral (D) view. Dorsal osteoderm with the typical anterior process (E). Scale bar 5 cm.

APPENDIX 2.

Character scoring from Martin et al. (2014) together with the Monteviale taxon included.

Polymorphic characters are indicated by the following letters: A=[01], B=[02], C=[12], D= [15].

Bernissartia fagesii

??????0???0111102100?00?0?000???0000?100010???0010?000???????10?0?00?001?1????000?0?0000?00030?00?????1000????1?0000?000??0100?0??000100?0?0??0?0?0010?0??00??0????????000?0000?000

Allodaposuchus precedens

??00010?000000123000000?100000????000000010103000110001011 00???0100000001100010000?????1??01?010001?000

Acynodon iberoccitanus

??1010410 1????????0????????0?0?????00010?00000010600000??00100????0000000101?00???20000?0100?110?0000??010100000?1?????????1??0????010

Acynodon adriaticus

?????1?????????????01?100?1??????????010?10?????????01????????0???0??100??00??00010?000?0?1060000?0????110????00?00011010000?1?11?0?0100???0????0??010?0?0010?????????????1???01?0

Iharkutosuchus makadii

??10124?????????110???00??10?1????0001??00000110610 00?0???0110????0000001001100001201001?100?1?0?00?0???12???100?2?????1???1000000??110

Hylaeochampsa vectiana

??0?????0??????????0

?0?1000?00??0110?0?0000000?1001000?0?2110000120????1?0?000010100000000????1?001001000?0110

Eothoracosaurus mississippiensis

??????0????????????01??000????????00?00???0????122????3??????0?????00?011?0????00120?000??102500000??000000????000010100100????00?000100???01???1000001 0?001?00????????1000010000000

Thoracosaurus neocesariensis

??????0??????111?1?010????0011??0??0?00???0???1122????3????????10?000?01?0?????00120?0000?1025000000??000000?0?000010100100 00?000000011 0?00010??1?000010000100000000?00100?10000000

Thoracosaurus macrorhyncus

??????0???0?1111?1?01?????00????0????00???0???1?22????3??????0?100000001100????00120?00?0?1025000000??000000?0?000010100100001100000000110?000100?1000101 0?0010000???0??0100010000000

Eosuchus minor

??????0???0??111???01?00?0?01???0000?000??0???1122??0300?0000?10?000001100????00120?0000?1025?00000?000000?00000001010010000?100000001 10???0100?10?10010000 1?0100??1??101010101003

Eosuchus lerichei

??????0??????01????01???????1????????0????????1122????3??????????????????0?????00120?0000?1025000000?0000000???000010100100000100000?0110?000?0??10?200100001 0?1????????01?101003

Eogavialis africanum

????????1?????11???010??????????0?????????0???1122??03?????10?100000??1101????00120?00
0?01025?00000?0000000000000010100100000100000000121?000100?1001001000010100?000??0
101010100000

Piscogavialis jugaliperforatus

??????????????????????????????1?????????????11?2???3?????0001???????10??????00120?001
001025000000?000000????00001010010000000?000000111?1?00010100200100000200?0?1?0?0?1
2??1?10?000

Gryposuchus colombianus

????0?0???001??????01??000???????????????0???11223?030100?00010000000110 0????001201
0000?1025?00000?0?0000??0?00001010010000011000000121?000100?10011010000200000100?
00121010100000

Gavialis lewisi

???????????????????010??????????????????????????22???3??????0?100000??1?0?????00?30?0??
????2??0???0?0?0000??0?0000?0?00100?0?1???0000121?000100?100??0?000010000?????00121
010100000

Gavialis gangeticus

020000000?00111101101000000011100000 0?000000001122300300000000100000001100010000
1301000001025?0000000000000000000010100100000110000001210000100010011010000100 00
0000000121010100000

Borealosuchus threensis

????0??????????????01???????0??????1?00??20???01002??1?????10?11?000001000???????????
??
???

Borealosuchus formidabilis

000?000?0?1100100100100000010100000 1?000?20???0110200000?000?110000000100001??000

20?0000?00231000000?0000001000000010100100010100201?11000000?00?00001010010100000?
???00100110000000

Borealosuchus wilsoni

??????0??????????10010000001010??00?1?000?20???01002??100?0?00110000020100000?000020?
0?0???0231000?????00001?0?0?00101001000101002010110 0?000100??00110100101000 0?00???
010011?0?0000

Borealosuchus acutidentatus

??????????????????????????????0??????????????????002????????????000??????0?????00020?0?00
??0231000?????0000????0?0??0???????1??002?1?1100?0?0?0??0?011010?101000???????010??1?
0?0000

Borealosuchus sternbergii

000000000?110010?100100000010100000 1?00???0???01102000000?000100000001000000??000
20?000000013100000010000 01?0?00000111010001010000111100?000100?00000010010100000
0?1?00100110000000

Pristichampsus vorax

????0?0???01001001?01?00000111??0100?10???1???1110?000?????0??1000001?1?0?????21010?
0000?0003000100?000000??0?000000100100010100001111 10???0100?0100001001010 00???01?
?1100110000002

Pristichampsus geiseltalensis

?????????????0?0???01?000?0??1??0100?1???1????11102000??????0?1????0??1?1?????21?20?00
00000030001???000000????000000100101 0??10000111110?0?0?00?0?010010?10100?????????1?
??10000002

Planocrania hendongensis

??????????????????1?????????????????????????1110???1????????1????0?01?0?????20010?0???
??01300??????0?000????0????01001???????0??1?1100????????0?0?00100?0100?????1???1???10
?10001

Planocrania

datangensis??11?????0??????????????????????????2

0010?000??1003000000??0?000???????000??01???????0??1?1110????????0?00001001O??0??????

???????10??0?0?

Leydiosuchus canadensis

????0?0????????1????0100000011?1??10?0?11??11???0110?00000?0?01?10000001110l????00010?

000000003000000000100010001000011101000101000011110O?0101001001000100101000000001

?00100110010001

Deinosuchus riograndensis

??????0????????????01??????????????????00???1???0110???001?0?11?10??0??11?0?????00??1?0??

????0?0000???0??00011?00?0?????????????????0001111120?012210?1110001001?1000??000?0?????

1??100?1

Diplocynodon ratelii

??????0??????000???010?00?1111001400?10??21???0100210l?????0111000001?1101????00120?

000000123000000010000O??0?000000111100010100001111OO??10100100000010110100000001

?10100110010001

Monteviale

??????????0??????0?01?0???1??????4?0?101?20?????0????[12]??????????????1???????

?00120?100000??3??00???????00?????0?00?1?11?0??0100001?1100???0????0??0101?11010

0????????????0?10?10001

Diplocynodon

*hantoniensis*100???1?1?0100001000100001111l??1400?101?21???01102101O????0111000001111

01????00120?0?000?11300?000?1000001?0?000000101100010100001111OO?110100?001010101

101000??0?1??010011?010001

Diplocynodon

muelleri??????????????????????1?01??1?????14?0?10??21???01002????????01110??10011100????0

0120?10000012300000001000000????0000011111000001000?1?1100?110??0?01?01010110100???
?????0100110010001

Diplocynodon tormis

??????????????????????1?????1??????????10??21???01?021?1?????01?1?00????11??????0?120??00
000123000000?1010001???000000111100?0?10000111100?1101000001010101101000?0???1?001
?0110010001

Diplocynodon

*darwini*10000100 1?010000?00010000?1111??1400?101121???01102001 0??0?01?1000001111010
0??00020?0000?0103000000?0??000??0?0000001111?00101000?111100?110100?011010101101
000???????0100110010001

Diplocynodon deponiae

100?0?0???????0????01?0???1?????14?0?10??21????1?02??0?????01?10??0??1110?????001???00
0??01030000?0???1000?????0?0001?11000?01000?111100?110100?0??011?0?101?00????????1?
??1??10001

Brachychampsa montana

101011001?1100???0001??000111100?000?103111???1110110 1?????01110?00001110100??0011
0?0002?1101000000?0010001?0?0100000111100101200111 1100?110200?0111001011010200010
1?00100110010001

Brachychampsa sealeyi

??????????????????????????????????????10???1???11101??0???????11??0000111?1????001?0?000
2?110100000???010?????????00????????10?2001101?00???????????100???????2?????????????1?
?10??1

Stangerochampsa mccabei

????110???010010?000100000111100100 0?01??11???1110101 00????0111110000?110?????00110
?0002?1102000000?001000????000000011110010120011111 00?110200?0?1100102101000??1?1
??0100110010001

Ceratosuchus burdoshi

????????????????????????????????????0?1????????11111??0?????01?10??00?11?01????00010?0?0
1?0102000000???1000??0????00???01???1?1??0?111100????????0????010?111???????????10??1
0010001

Hassiacosuchus haupti

001?1?0?1??????0???01?000?1111?????0??11?11???111110?0?????01?10??0??11101????00010?
00???010?0000??????0001?0??????0?????????1100?111100?1?0200?01120010210101????????01
???10010001

Navajosuchus mooki

??????0?1??????0???0?00???1111??1??0?111111???1111010?????01?10??00??110?????00010?0
001?01020000???0?1000??0???00?00?1110010110011111100???020??0112?0102101000????1??01
0??10010001

Allognathosuchus

polyodon??1111101?????01?11??00?111?1????0
0010?000??0102000?0?????00??0?00?00?0?111001?1?01?111100????????0??20010?101???????
????1???1??1???1

Allognathosuchus wartheni

????1?0????????????0?0000?1111??1000?11???1???11111010?100?01111000001110 1????00010?
0000?0102000000000010001?0?000000?0111001?1101111110 0?110200?01120010210100 00?1?1?
0010011001?001

Procaimanoidea kayi

????110?1??????0???010?00?1111??10?0?112121?????010?1??100?01?1100000111 0?????10????
?0???010?0000???0?1000??0?000000000111 00?0110111111000??0200?01120010210101 0???????
0100110010001

Procaimanoidea utahensis

??110100?00??0101111 0??0011101????10110?01

00?01020?0000??01000????0000000?1110010110 1?111100?1?0200?0112001 0?101000???????01
00110010001

Arambourgia gaudryi

??11010??0?????01?100?0??1110?????1001??010
??0102000 0?0???10001000??000????11?0??1101?111100?1102?0?0?1210?0210100?????????100
11?010?01

Wannaganosuchus brachymanus

????1?0???1?00?0???010000?1111001000?11???1???111110?0?????0??100?00?11?0?????00110?
0000??10200??00???1000??0?100000???1??01?1101?111100????????0?12001??101000????????1
0011?010001

Alligator sinensis

101011101?1100101000101101111100110001121111101100001 20?00101120000011110 1??1100
1000010000102000000000100011001000000111100101101111111001102001011200102101010 0
0111100100110010001

Alligator mississippiensis

101011001?0100100000101101111100110001121011001100011201001011200010111101001100
1000010000102000000000100011100000000111100101101111111001102001011210102101010 0
0111100100110010001

Alligator

mefferdi??????????????????????????????1?????????11???????1100001201000011200010111101 00??
00100?0100?0102000000?0?10001?1?0000000?1110010110111111110?110200?011210102101010
??1???00100110010001

Alligator

thomsoni??????????????????????01????????1?????0?1????????110000?2?????0112000100111 01????
00100?0100001020 00?0??0010001?1?000000????1?????10111111110?1?0200101?2101021010 1?0
01?11?0100110010001

Alligator olseni??????0?1?????10???01?10011111???100?11???????1101001O?????0112000000111O1????0
0100?01000?10200??00???1000??0?0?000101111101011011111110?110200?0112001021010??
????00100?1?010001

*Alligator mcgrewi*100010001?010010?000100001111?1101??0?11???1???1111001O?100?0111000001111O1?
???00000?0100?0102000000?0010001?00100000011110010110111111000110200?011200102101
010?01???00100110010001

*Alligator prenasalis*10001?0?1?????10?0?0100001111??1000?112111???1111101O?????011100000111101
00??00000?0100?0102000000?00100011001000000111100101101111110O?110200?01120010210
1000001?1?00100110010001

Eocaiman cavernensis
??1110???2?????11?1??????????????00????0????
??0??????????100???0?1??0000???????0?????1??1?0?????0???????0??????1?3???????????0??1?2??
???

Tsoabichi greenriverensis
??????????????????????01??????????????????10??20???1100???2????????1??????11???01??00010?10?
???10??000????????0?????????????????????????000?1111?0?1?0????0??211???101?2?????????????????
100??

Purussaurus neivensis
101?100?1?000010?0??1????011???????0?11???1???1?00??1?1010?111201100011001????00110?
0001?0102000000?0010001?0?0?000001111012111111111110?110201?0112011?210102000101?
?010??10210001

Orthogenysuchus olseni

??00?????????????????????0?????00121?0?01?

?10?0?0???????000????01?000?????????????????11110????????0????11??101??0???????????????10

001

Mourasuchus spp.

10??100?1?00?010?00?1?10?011????1300?11???1???1102?112?????01110?10001100????00121

?0000?1105000100?0010001?0?0100000111101 2?1011?111110?110?00????2111??111?30????1?

??100110?10001

Caiman yacare

101111001?10001000001010111111001100011122111011002112101011101011020110010111001

1100000000112000000000100011001000000111101211110111111001102011011201112101030001

0101100100110210001

Caiman

*crocodilus*101111001?10001000001010111111001100011122111011002112101011101011020110

0101110011000000001120000000001000110010000001111012111001111110011020110112011121

2101030001011001001102100 01

Caiman latirostris

101110001?10001000001010?1111100110001112212101100211210101 11?10110201100???1100

1100000000102001000000100011001000000111101211100111111001102011011211112101030001

0101100100110210001

Caiman lutescens

??0??????????????????????????????00110?0000?

0102001000?001000????100000011110121120 0?1?1?10?????0???????1????0?????????????????

100?1

Melanosuchus fisheri

??????0????????0??????????????????????????????????02????????1?11011????10?1????001?0?000
0??10200101O???1000??0???0????11????2?11???111110????????0????11??1010??????????010??1
?2?0001

Melanosuchus niger

101111001?1?00100000101011111100110001112212101100211210101111101102011001??1100
11000000001020010100001000110010000001111012111001111110011020110112111121010300
0101100100110210001

Paleosuchus trigonatus

100111111?0100101000100011111121130001113211201100212221111111101100011001011110
11000010001020000000001000110001000101111011110001111110111020110112111?21010200
0101100100110210001

Paleosuchus

*palpebrosus*100111111?0100101010100011111121130001113211201100212221111?11?10110001
100?0111101100001000102000000000100011000100010111101111000111111011102011011211
1?2101020001011001001102100 01

Mecistops cataphractus

10?001001?0000100000111001111120120001111011011110410101000100100011101 01?100100
12000000100210000000100000110100001011010001010000111110000101110012001001010001
1101011110010000003

Crocodylus niloticus

101000001?1010100010111001111120120001112011011100210101000101100011101011100100
11000000100210000001100000110100100011010001011000111110000101110012001001010001
1101011110011000003

Crocodylus

*porosus*111000001?0010101010111000111120120001112011011100210101000101100011101011

100100110000001002100010011000001101001000110100010100001111100001011100120010010100011100111010111110011000003

*Crocodylus rhombifer*001000001?10101000101110011111201100011120110111002101010001011000111010111001001100000010021010000110000011010010001101000101100011111000010111001200100111010011101011110011000003

Euthecodon arambourgii

??0????????????????????1?????00020?00000?10250001 00?10000011010000000??0????0???000111110??11011?00121010010110 0????1??11?0?1000?003

Osteolaemus tetraspis

??1?00001?00101010001110011111201110011111111011100210101000101100001101011100110100000101002100010001000001101100101110101010100001111101001010100121110010110011101011110110000003

Osteolaemus osborni

??1?00001?00101010001110011111201110011111111011100210101000001100001101011100110110000101002100010001000001101100100100101010100001111101001010100121110010110011101011110110000003

Voay robustus

??????0????????0???011?????111??1110??????1???111021010100000110001111101 1????00110?0000?00210001000100000110100010111010101010000111110?00101110012011001111110?1101?11110010000003

Rimasuchus lloydi

??1????????????????????1?????00110?00000?00210001 00?10000011010000000????10??1??100?111110?001011?00120010010110011 1?1??1110?1000?003

Crocodylus pigotti

??????????00?010?00?11??01111????????10???0???11102??1????????1???111???1?????00010?01
00?00210001000100000????00101011010100 01?0?0111110???1?1??00121010010110 0??1?1??11
00?10000003

Crocodylus megarhinus

??????0???????????001?????????????????????????????1110210 1?????00110000??01011????00110?00
00?00230000000 1?0000??0?0000001101000101200011111 0?002?11?0012?0100101 0?01100???1
110010000003

Australosuchus clarkae

??????0???????1??0??1?????11????????0?10???1???1110?101?????00110000110101 1????00110?0
000110210000000 1000001?0?000000???????10100001111 0?002011?0112001001010001 1??1??1
1?001000?001

Kambara implexidens

??????0????????????01?????11????1100?10???1???1110210 1?????00110000110101 1????00110?0
000110210000000 1000001?0100000010010001010000111 10?002011?0012001001010001 11101?
11110010000001

Trilophosuchus rackhami

??0?????0?????
?2?0??0?0?1000????0?1?000001010???01?0?0111110??1201110112101000010201 1101?111?0?1
000?001

Quinkana spp.

??11?0???1?????????????????1?????21010?0000
?10[02][15]00[01]0000100000????0?0??????????1??1000111?10?0020111001210100 10102?1110
1?11??01?000???1

Tomistoma schlegelii

021000001?001010001011000111111011000101301101112 2?1040000010010000000101000010012000000110210000010100000110100010010010001011000111110000011010012101001010001100101111001000000 3

Tomistoma lusitanica??????0????????????01??????????????????10???1???1??2???4?????00?10000??0101?????00120?0000?1021?00001?10000011 0?000010100100010100001111 10?0001?1?101210100101000 11001??1110010000003

Toyotamaphimeia machikanense

00100100??1111110010110001111110110 0?00???1?????22??04?????10010?0000?101000??00120?0000110040000 0???00000????0000?010010000?1000001111 0??00?1??1??21010?1010????????110010?00003

Gavialosuchus eggemburgensis

??????????????????1??00120?0000?1024000000??00000????00?0101001000?01200?0?1110?0??????1?121010?10100????????11???10000003

Paratomistoma courti

??0??10?000001010????00????????????2??0?0??????0001?0??????????????????000?1??11?????1???1??200100001000?1000?101?0?100??00?

Tomistoma cairense??1??2???4????????1000001?1010????00?20?0?????025?0???0????000??0?000010100100010?00??011110???01???10?2001001010001??0???11?001?000003

Thecachampsa antiqua

02000000??001010?000110101111?1??11?0?00???1???1122???4?100????1000031?101?0???00120

?0000110210000000?100000??0?0000101?0100010110000111102??011??10120010010101O??00??111001002003

Tomistoma petrolica????????????????????????????1????????????????????????04?????0010?0?01?1?10????00???????????2?00?0?0???00001???0?00101001??????1?0?0?1110?0?2?0??0??200?00001002??????????1???1????003

Dollosuchus densmorei

001???0???111010?0001?0?001111??1?00??????????1120???0?????000100?0??0101?????00120?00?0?1021000000??00000????01?0101001000101100?011110????????1??20010?1010001???????10?01000?003

Kentisuchus spenceri

??????0??1?????0?????0??1000?1101?11????00110?0000?1021000000???0000??0?0100101001001?01100?111110??????0?0??20010?10100???????111?0?100?0?03

Brachyuranocampsa eversolei

??0011??00???1021000000??00000??0?0?0??01101000101000?111100???2?00?0?121010?101000???????110001000003

"*Crocodylus*" acer

??00110?0000?1021000000??000001???000100?10100010100001111002?002?01?00?2001001010001??0??11100010000003

Asiatosuchus depresifrons

???00?00??110000100111000011112??1100?10???1???1110210?????00110000000101l????00110?0000?1011000000?1100001?0?0001001?01000101?000111100?010200?00120010010100011001?11100010000003

"*Crocodylus*" *affinis*

001001001?10001000011100001111001100?10???1???11102101010000011000000010110 0??001 10?000010011000000?010000??0?000100110100010100001111 00?0?010??00120010010100 01??0???1100010000003

Asiatosuchus germanicus

001?0?0?1?001010?0101?000?1111??1??0??????1???11102000?????00110000??0101?00??00010 ?0000?000100000???10000??0?00010???0100010100 0?111100???0100?00111010010100 0??????1100?10000003

Prodiplocynodon langi

??00110?0000? ?003000000??100001??000010011?1000101????111100???0?0??0?11?010?1010001??01?011001 10000003

Diplocynodon remensis

????????????????????????????????????10??20???0100200 0?????01110?000111001????00?20?00 000001310000001 00???1???0000001101000101000 01?1100???0100000001010110100???1?1??01 00110010001

APPENDIX 3.

Character description from Brochu et al. (2012).

(1) Ventral tubercle of proatlas more than one-half (0) or no more than one half (1) the width of the dorsal crest.

(2) Fused proatlas boomerang-shaped (0), strap-shaped (1), or massive and block-shaped (2).

(3) Proatlas with prominent anterior process (0) or lacks anterior process (1).

(4) Proatlas has tall dorsal keel (0) or lacks tall dorsal keel; dorsal side smooth (1).

(5) Atlas intercentrum wedge-shaped in lateral view, with insignificant parapophyseal processes (0), or plate-shaped in lateral view, with prominent parapophyseal processes at maturity (1).

(6) Dorsal margin of atlantal rib generally smooth with modest dorsal process (0) or with prominent process (1).

(7) Atlantal ribs without (0) or with (1) very thin medial laminae at anterior end.

(8) Atlantal ribs lack (0) or possess (1) large articular facets at anterior ends for each other.

(9) Axial rib tuberculum wide, with broad dorsal tip (0) or narrow, with acute dorsal tip (1).

(10) Axial rib tuberculum contacts diapophysis late in ontogeny, if at all (0) or early in ontogeny (1).

(11) Anterior half of axis neural spine oriented horizontally (0) or slopes anteriorly (1).

(12) Axis neural spine crested (0) or not crested (1).

(13) Posterior half of axis neural spine wide (0) or narrow (1).

(14) Axis neural arch lacks (0) or possesses (1) a lateral process (diapophysis).

(15) Axial hypapophysis located toward the center of centrum (0) or toward the anterior end of centrum (1).

(16) Axial hypapophysis without (0) or with (1) deep fork.

(17) Hypapophyseal keels present on eleventh vertebra behind atlas (0), twelfth vertebra behind atlas (1), or tenth vertebra behind atlas (2).

(18) Third cervical vertebra (first postaxial) with prominent hypapophysis (0) or lacks prominent hypapophysis (1).

(19) Neural spine on third cervical long, dorsal tip at least half the length of the centrum without the cotyle (0) or short, dorsal tip acute and less than half the length of the centrum without the cotyle (1).

(20) Cervical and anterior dorsal centra lack (0) or bear (1) deep pits on the ventral surface of the centrum.

(21) Presacral centra amphicoelous (0) or procoelous (1).

(22) Anterior sacral rib capitulum projects far anteriorly of tuberculum and is broadly visible in dorsal view (0), or anterior margins of tuberculum and capitulum nearly in same plane, and capitulum largely obscured dorsally (1).

(23) Scapular blade flares dorsally at maturity (0) or sides of scapular blade sub-parallel; minimal dorsal flare at maturity (1).

(24) Deltoid crest of scapula very thin at maturity, with sharp margin (0) or very wide at maturity, with broad margin (1).

(25) Scapulocoracoid synchondrosis closes very late in ontogeny (0) or relatively early in ontogeny (1).

(26) Scapulocoracoid facet anterior to glenoid fossa uniformly narrow (0) or broad immediately anterior to glenoid fossa, and tapering anteriorly (1).

(27) Proximal edge of deltopectoral crest emerges smoothly from proximal end of humerus and is not obviously concave (0) or emerges abruptly from proximal end of humerus and is obviously concave (1).

(28) M. teres major and M. dorsalis scapulae insert separately on humerus; scars can be distinguished dorsal to deltopectoral crest (0) or insert with common tendon; single insertion scar (1).

(29) Olecranon process of ulna narrow and sub-angular (0) or wide and rounded (1).

(30) Distal extremity of ulna expanded transversely with respect to long axis of bone; maximum width equivalent to that of proximal extremity (0) or proximal extremity considerably wider than distal extremity (1).

(31) Interclavicle flat along length, without dorsoventral flexure (0), or with moderate dorsoventral flexure (1), or with severe dorsoventral flexure (2).

(32) Anterior end of interclavicle flat (0) or rod-like (1).

(33) Iliac anterior process prominent (0) or virtually absent (1).

(34) Dorsal margin of iliac blade rounded with smooth border (0) or rounded, with modest dorsal indentation (1) or rounded, with strong dorsal indentation (wasp-waisted; 2) or narrow, with dorsal indentation (3) or rounded with smooth border; posterior tip of blade very deep (4).

(35) Supraacetabular crest narrow (0) or broad (1).

(36) Limb bones relatively robust, and hind limb much longer than forelimb at maturity (0) or limb bones very long and slender (1).

(37) M. caudofemoralis with single head (0) or with double head (1).

(38) Dorsal osteoderms not keeled (0) or keeled (1).

(39) Dorsal midline osteoderms rectangular (0) or nearly square (1).

(40) Four (0), six (1), eight (2), or ten (3) contiguous dorsal osteoderms per row at maturity.

(41) Nuchal shield grades continuously into dorsal shield (0), or differentiated from dorsal shield; four nuchal osteoderms (1), or differentiated from dorsal shield; six nuchal osteoderms with four central and two lateral (2), or differentiated from dorsal shield; eight nuchal osteoderms in two parallel rows (3).

(42) Ventral armor absent (0), or single ventral osteoderms (1), or paired ventral ossifications that suture together (2).

(43) Anterior margin of dorsal midline osteoderms with anterior process (0) or smooth, without process (1).

(44) Ventral scales have (0) or lack (1) follicle gland pores.

(45) Ventral collar scales not enlarged relative to other ventral scales (0), or in a single enlarged row (1), or in two parallel enlarged rows (2).

(46) Median pelvic keel scales form two parallel rows along most of tail length (0), or form single row along tail (1), or merge with lateral keel scales (2).

(47) Alveoli for dentary teeth 3 and 4 nearly same size and confluent (0) or fourth alveolus larger than third, and alveoli are separated (1).

(48) Anterior dentary teeth strongly procumbent (0) or project anterodorsally (1).

(49) Dentary symphysis extends to fourth or fifth alveolus (0), or sixth through eighth alveolus (1), or behind eighth alveolus (2)

(50) Dentary gently curved (0), deeply curved (1), or linear (2) between fourth and tenth alveoli.

(51) Largest dentary alveolus immediately caudal to fourth is (0) 13 or 14, (1) 13 or 14 and a series behind it, (2) 11 or 12, or (3) no differentiation, or (4) behind 14

(52) Splenial with anterior perforation for mandibular ramus of cranial nerve V (0) or lacks anterior perforation for mandibular ramus of cranial nerve V (1)

(53) Mandibular ramus of cranial nerve V exits splenial anteriorly only (0), or splenial has singular perforation for mandibular ramus of cranial nerve V posteriorly (1), or splenial has double perforation for mandibular ramus of cranial nerve V posteriorly (2).

(54) Splenial participates in mandibular symphysis; splenial symphysis adjacent to no more than five dentary alveoli (0) or splenial excluded from mandibular symphysis; anterior tip of splenial passes ventral to Meckelian groove (1) or splenial excluded from mandibular symphysis; anterior tip of splenial passes dorsal to Meckelian groove (2) or deep splenial symphysis, longer than five dentary alveoli; splenial forms wide 'V' within symphysis (3) or deep splenial symphysis, longer than five dentary alveoli; splenial constricted within symphysis and forms narrow V (4).

(55) Coronoid bounds posterior half of foramen intermandibularis medius (0) or completely surrounds foramen intermandibularis medius at maturity (1), or obliterates foramen intermandibularis medius at maturity (2).

(56) Superior edge of coronoid slopes strongly anteriorly (0) or almost horizontal (1).

(57) Inferior process of coronoid laps strongly over inner surface of Meckelian fossa (0) or remains largely on medial surface of mandible (1).

(58) Coronoid imperforate (0) or with perforation posterior to foramen intermandibularis medius (1).

(59) Process of splenial separates angular and coronoid (0) or no splenial process between angular and coronoid (1).

(60) Angular-surangular suture contacts external mandibular fenestra at posterior angle at maturity (0) or passes broadly along ventral margin of external mandibular fenestra late in ontogeny (1).

(61) Anterior processes of surangular unequal (0) or sub-equal to equal (1).

(62) Surangular with spur bordering the dentary tooth row lingually for at least one alveolus length (0) or lacking such spur (1).

(63) External mandibular fenestra absent (0) or present (1) or present and very large; most of foramen intermandibularis caudalis visible in lateral view (2).

(64) Surangular-dentary suture intersects external mandibular fenestra anterior to posterodorsal corner (0) or at posterodorsal corner (1).

(65) Angular extends dorsally toward or beyond anterior end of foramen intermandibularis caudalis; anterior tip acute (0) or does not extend dorsally beyond anterior end of foramen intermandibularis caudalis; anterior tip very blunt (1).

(66) Surangular-angular suture lingually meets articular at ventral tip (0) or dorsal to tip (1).

(67) Surangular continues to dorsal tip of lateral wall of glenoid fossa (0) or truncated and not continuing dorsally (1).

(68) Articular-surangular suture simple (0) or articular bears anterior lamina dorsal to lingual foramen (1) or articular bears anterior lamina ventral to lingual foramen (2), or bears laminae above and below foramen (3).

(69) Lingual foramen for articular artery and alveolar nerve perforates surangular entirely (0) or perforates surangular/angular suture (1).

(70) Foramen aerum at extreme lingual margin of retroarticular process (0) or set in from margin of retroarticular process (1).

(71) Retroarticular process projects posteriorly (0) or projects posterodorsally (1).

(72) Surangular extends to posterior end of retroarticular process (0) or pinched off anterior to tip of retroarticular process (1).

(73) Surangular-articular suture oriented anteroposteriorly (0) or bowed strongly laterally (1) within glenoid fossa.

(74) Sulcus between articular and surangular (0) or articular flush against surangular (1).

(75) Dorsal projection of hyoid cornu flat (0) or rodlike (1).

(76) Dorsal projection of hyoid cornu narrow, with parallel sides (0) or flared (1).

(77) Lingual osmoregulatory pores small (0) or large (1).

(78) Tongue with (0) or without (1) keratinized surface.

(79) Teeth and alveoli of maxilla and/or dentary circular in cross-section (0), or posterior teeth laterally compressed (1), or all teeth compressed (2)

(80) Maxillary and dentary teeth with smooth carinae (0) or serrated (1).

(81) Naris projects anterodorsally (0) or dorsally (1).

(82) External naris bisected by nasals (0) or nasals contact external naris, but do not bisect it (1), or nasals excluded, at least externally, from naris; nasals and premaxillae still in contact (2), or nasals and premaxillae not in contact (3).

(83) Naris circular or keyhole-shaped (0), or wider than long (1), or anteroposteriorly long and prominently teardrop-shaped (2).

(84) External naris of reproductively mature males (0) remains similar to that of females or (1) develops bony excrescence (ghara).

(85) External naris (0) opens flush with dorsal surface of premaxillae or (1) circumscribed by thin crest.

(86) Premaxillary surface lateral to naris smooth (0) or with deep notch lateral to naris (1).

(87) Premaxilla has five teeth (0) or four teeth (1) early in post-hatching ontogeny.

(88) Incisive foramen small, less than half the greatest width of premaxillae (0), or large, more than half the greatest width of premaxillae (1), or large, and intersects premaxillary-maxillary suture (2).

(89) Incisive foramen completely situated far from premaxillary tooth row, at the level of the second or third alveolus (0), or abuts premaxillary tooth row (1), or projects between first premaxillary teeth (2).

(90) Dorsal premaxillary processes short, not extending beyond third maxillary alveolus (0) or long, extending beyond third maxillary alveolus (1).

(91) Dentary tooth 4 occludes in notch between premaxilla and maxilla early in ontogeny (0) or occludes in a pit between premaxilla and maxilla; no notch early in ontogeny (1).

(92) All dentary teeth occlude lingual to maxillary teeth (0) or occlusion pit between seventh and eight maxillary teeth; all other dentary teeth occlude lingally (1), or dentary teeth occlude in line with maxillary tooth row (2).

(93) Largest maxillary alveolus is 3 (0), 5 (1), 4 (2), 4 and 5 are same size (3), 6 (4), or maxillary teeth homodont (5), or maxillary alveoli gradually increase in diameter posteriorly toward penultimate alveolus (6).

(94) Maxillary tooth row curved medially or linear (0) or curves laterally broadly (1) posterior to first six maxillary alveoli.

(95) Dorsal surface of rostrum curves smoothly (0) or bears medial dorsal boss (1).

(96) Canthi rostralii absent or very modest (0) or very prominent (1) at maturity.

(97) Preorbital ridges absent or very modest (0) or very prominent (1) at maturity.

(98) Vomer entirely obscured by premaxilla and maxilla (0) or exposed on palate at premaxillary-maxillary suture (1).

(99) Vomer entirely obscured by maxillae and palatines (0) or exposed on palate between palatines (1).

(100) Surface of maxilla within narial canal imperforate (0) or with a linear array of pits (1).

(101) Medial jugal foramen small (0) or very large (1).

(102) Maxillary foramen for palatine ramus of cranial nerve V small or not present (0) or very large (1).

(103) Ectopterygoid abuts maxillary tooth row (0) or maxilla broadly separates ectopterygoid from maxillary tooth row (1).

(104) Maxilla terminates in palatal view anterior to lower temporal bar (0) or comprises part of the lower temporal bar (1).

(105) Penultimate maxillary alveolus less than (0) or more than (1) twice the diameter of the last maxillary alveolus.

(106) Prefrontal dorsal surface smooth adjacent to orbital rim (0) or bearing discrete knoblike processes (1).

(107) Dorsal half of prefrontal pillar narrow (0) or expanded anteroposteriorly (1).

(108) Medial process of prefrontal pillar expanded dorsoventrally (0) or anteroposteriorly (1).

(109) Prefrontal pillar solid (0) or with large pneumatic recess (1).

(110) Medial process of prefrontal pillar wide (0) or constricted (1) at base.

(111) Maxilla has linear medial margin adjacent to suborbital fenestra (0) or bears broad shelf extending into fenestra, making lateral margin concave (1).

(112) Anterior face of palatine process rounded or pointed anteriorly (0) or notched anteriorly (1).

(113) Anterior ectopterygoid process tapers to a point (0) or forked (1).

(114) Palatine process extends (0) or does not extend (1) significantly beyond anterior end of suborbital fenestra.

(115) Palatine process generally broad anteriorly (0) or in form of thin wedge (1).

(116) Lateral edges of palatines smooth anteriorly (0) or with lateral process projecting from palatines into suborbital fenestrae (1).

(117) Palatine-pterygoid suture nearly at (0) or far from (1) posterior angle of suborbital fenestra.

(118) Pterygoid ramus of ectopterygoid straight, posterolateral margin of suborbital fenestra linear (0) or ramus bowed, posterolateral margin of fenestra concave (1) (rephrased from original).

(119) Lateral edges of palatines parallel posteriorly (0) or flare posteriorly, producing shelf (1).

(120) Anterior border of the choana is comprised of the palatines (0) or choana entirely surrounded by pterygoids (1).

(121) Choana projects posteroventrally (0) or anteroventrally (1) at maturity.

(122) Pterygoid surface lateral and anterior to internal choana flush with choanal margin (0), or pushed inward anterolateral to choanal aperture (1), or pushed inward around choana to form neck surrounding aperture (2), or everted from flat surface to form neck surrounding aperture (3).

(123) Posterior rim of internal choana not deeply notched (0) or deeply notched (1).

(124) Internal choana not septate (0), or with septum that remains recessed within choana (1), or with septum that projects out of choana (2).

(125) Ectopterygoid-pterygoid flexure disappears during ontogeny (0) or remains throughout ontogeny (1).

(126) Ectopterygoid extends (0) or does not extend (1) to posterior tip of lateral pterygoid flange at maturity.

(127) Lacrimal makes broad contact with nasal; no posterior process of maxilla (0), or maxilla with posterior process within lacrimal (1), or maxilla with posterior process between lacrimal and prefrontal (2).

(128) Prefrontals separated by frontals and nasals (0) or prefrontals meet medially (1).

(129) Lacrimal longer than prefrontal (0), or prefrontal longer than lacrimal (1), or lacrimal and prefrontal both elongate and nearly the same length (2).

(130) Ectopterygoid extends along medial face of postorbital bar (0) or stops abruptly ventral to postorbital bar (1).

(131) Postorbital bar massive (0) or slender (1).

(132) Postorbital bar bears process that is prominent, dorsoventrally broad, and divisible into two spines (0) or bears process that is short and generally not prominent (1).

(133) Ventral margin of postorbital bar flush with lateral jugal surface (0) or inset from lateral jugal surface (1).

(134) Postorbital bar continuous with anterolateral edge of skull table (0) or inset (1).

(135) Margin of orbit flush with skull surface (0), or dorsal edges of orbits upturned (1), or orbital margin telescoped (2).

(136) Ventral margin of orbit circular (0) or with prominent notch (1).

(137) Palpebral forms from single ossification (0) or from multiple ossifications (1).

(138) Quadratojugal spine prominent at maturity (0) or greatly reduced or absent at maturity (1).

(139) Quadratojugal spine low, near posterior angle of infratemporal fenestra (0) or high, between posterior and superior angles of infratemporal fenestra (1).

(140) Quadratojugal forms posterior angle of infratemporal fenestra (0), or jugal forms posterior angle of infratemporal fenestra (1), or quadratojugal-jugal suture lies at posterior angle of infratemporal fenestra (2).

(141) Postorbital neither contacts quadrate nor quadratojugal medially (0), or contacts quadratojugal, but not quadrate, medially (1), or contacts quadrate and quadratojugal at dorsal angle of infratemporal fenestra (2), or contacts quadratojugal with significant descending process (3).

(142) Quadratojugal bears long anterior process along lower temporal bar (0) or bears modest process, or none at all, along lower temporal bar (1).

(143) Quadratojugal extends to superior angle of infratemporal fenestra (0) or does not extend to superior angle of infratemporal fenestra; quadrate participates in fenestra (1).

(144) Postorbital-squamosal suture oriented ventrally (0) or passes medially (1) ventral to skull table.

(145) Dorsal and ventral rims of squamosal groove for external ear valve musculature parallel (0) or squamosal groove flares anteriorly (1).

(146) Squamosal-quadrate suture extends dorsally along posterior margin of external auditory meatus (0) or extends only to posteroventral corner of external auditory meatus (1).

(147) Posterior margin of otic aperture smooth (0) or bowed (1).

(148) Frontoparietal suture deeply within supratemporal fenestra; frontal prevents broad contact between postorbital and parietal (0), or suture makes modest entry into supratemporal fenestra at maturity; postorbital and parietal in broad contact (1), or suture on skull table entirely (2).

(149) Frontoparietal suture concavoconvex (0) or linear (1) between supratemporal fenestrae.

(150) Supratemporal fenestra with fossa; dermal bones of skull roof do not overhang rim at maturity (0), or dermal bones of skull roof overhang rim of supratemporal fenestra near maturity (1), or supratemporal fenestra closes during ontogeny (2).

(151) Shallow fossa at anteromedial corner of supratemporal fenestra (0) or no such fossa; anteromedial corner of supratemporal fenestra smooth (1).

(152) Medial parietal wall of supratemporal fenestra imperforate (0) or bearing foramina (1).

(153) Parietal and squamosal widely separated by quadrate on posterior wall of supratemporal fenestra (0), or parietal and squamosal approach each other on posterior wall of supratemporal fenestra without actually making contact (1), or parietal and squamosal meet along posterior wall of supratemporal fenestra (2).

(154) Skull table surface slopes ventrally from sagittal axis (0) or planar (1) at maturity.

(155) Posterolateral margin of squamosal horizontal or nearly so (0) or upturned to form a discrete horn (1).

(156) Mature skull table with broad curvature; short posterolateral squamosal rami along paroccipital process (0) or with nearly horizontal sides; significant posterolateral squamosal rami along paroccipital process (1).

(157) Squamosal does not extend (0) or extends (1) ventrolaterally to lateral extent of paroccipital process.

(158) Supraoccipital exposure on dorsal skull table small (0), absent (1), large (2), or large such that parietal is excluded from posterior edge of table (3).

(159) Anterior foramen for palatine ramus of cranial nerve VII ventrolateral (0) or ventral (1) to basisphenoid rostrum.

(160) Sulcus on anterior braincase wall lateral to basisphenoid rostrum (0) or braincase wall lateral to basisphenoid rostrum smooth; no sulcus (1).

(161) Basisphenoid not exposed extensively (0) or exposed extensively (1) on braincase wall anterior to trigeminal foramen.

(162) Extensive exposure of prootic on external braincase wall (0) or prootic largely obscured by quadrate and laterosphenoid externally (1).

(163) Laterosphenoid bridge comprised entirely of laterosphenoid (0) or with ascending process or palatine (1).

(164) Capitate process of laterosphenoid oriented laterally (0) or anteroposteriorly (1) toward midline.

(165) Parietal with recess communicating with pneumatic system (0) or solid, without recess (1).

(166) Significant ventral quadrate process on lateral braincase wall (0) or quadrate-pterygoid suture linear from basisphenoid exposure to trigeminal foramen (1).

(167) Lateral carotid foramen opens lateral (0) or dorsal (1) to basisphenoid at maturity.

(168) External surface of basioccipital ventral to occipital condyle oriented posteroventrally (0) or posteriorly (1) at maturity.

(169) Posterior pterygoid processes tall and prominent (0), or small and project posteroventrally (1), or small and project posteriorly (2).

(170) Basisphenoid thin (0) or anteroposteriorly wide (1) ventral to basioccipital.

(171) Basisphenoid not broadly exposed ventral to basioccipital at maturity; pterygoid short ventral to median eustachian opening (0) or basisphenoid exposed as broad sheet ventral to basioccipital at maturity; pterygoid tall ventral to median eustachian opening (1).

(172) Exoccipital with very prominent boss on paroccipital process; process lateral to cranioquadrate opening short (0) or exoccipital with small or no boss on paroccipital process; process lateral to cranioquadrate opening long (1).

(173) Lateral eustachian canals open dorsal (0) or lateral (1) to medial eustachian canal.

(174) Exoccipitals terminate dorsal to basioccipital tubera (0), or send robust process ventrally and participate in basioccipital tubera (1), or send slender process ventrally to basioccipital tubera (2).

(175) Quadrate foramen aerum on mediodorsal angle (0) or on dorsal surface (1) of quadrate.

(176) Quadrate foramen aereum is small (0), comparatively large (1), or absent (2) at maturity.

(177) Quadrate lacks (0) or bears (1) prominent, mediolaterally thin crest on dorsal surface of ramus.

(178) Attachment scar for posterior mandibular adductor muscle on ventral surface of quadrate ramus forms modest crests (0) or prominent knob (1).

(179) Quadrate with small, ventrally-reflected medial hemicondyle (0) or with small medial hemicondyle; dorsal notch for foramen aerum (1), or with prominent dorsal projection between hemicondyles (2), or with expanded medial hemicondyle (3).


A
B

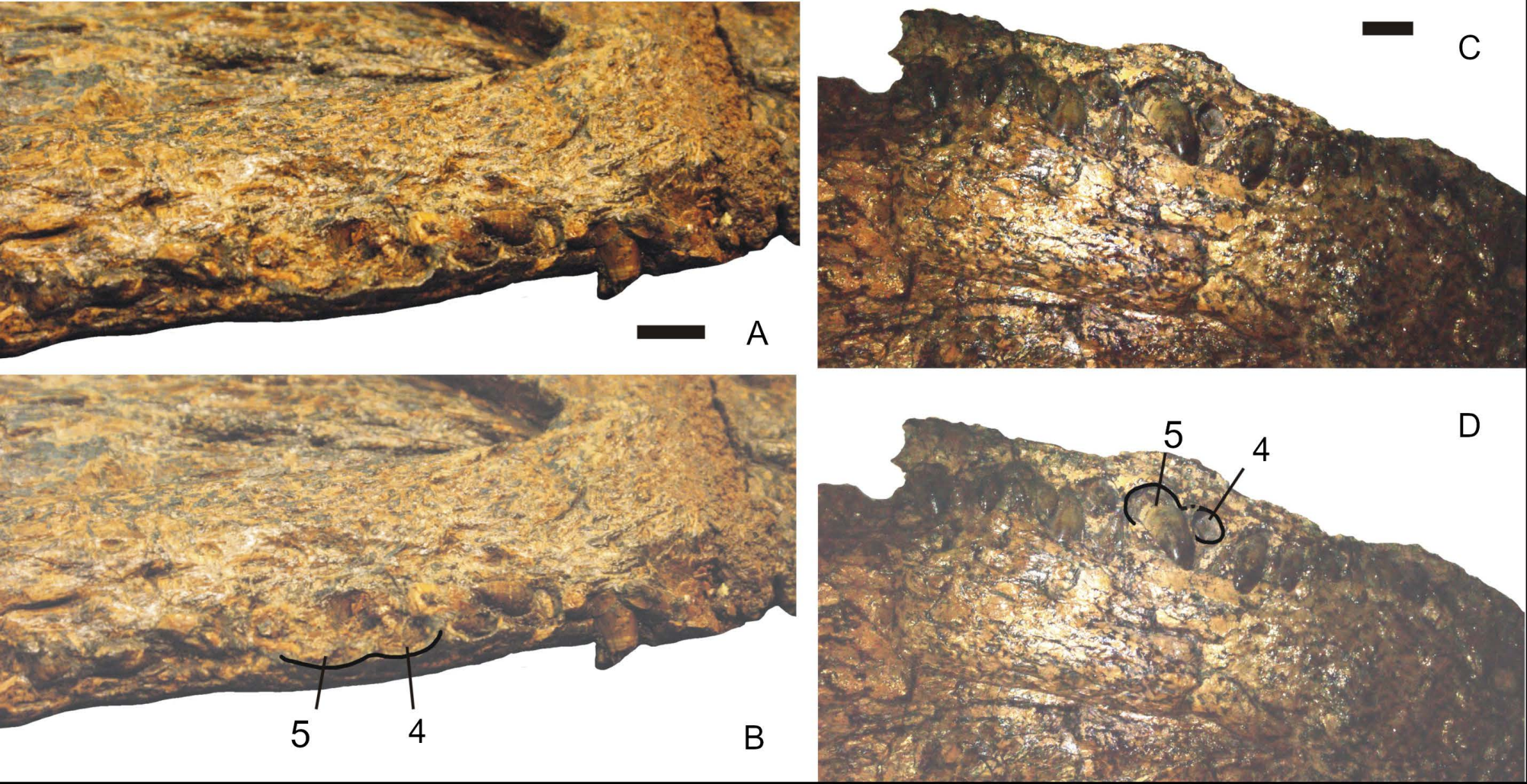
A
B
5
4
C
D
5
4

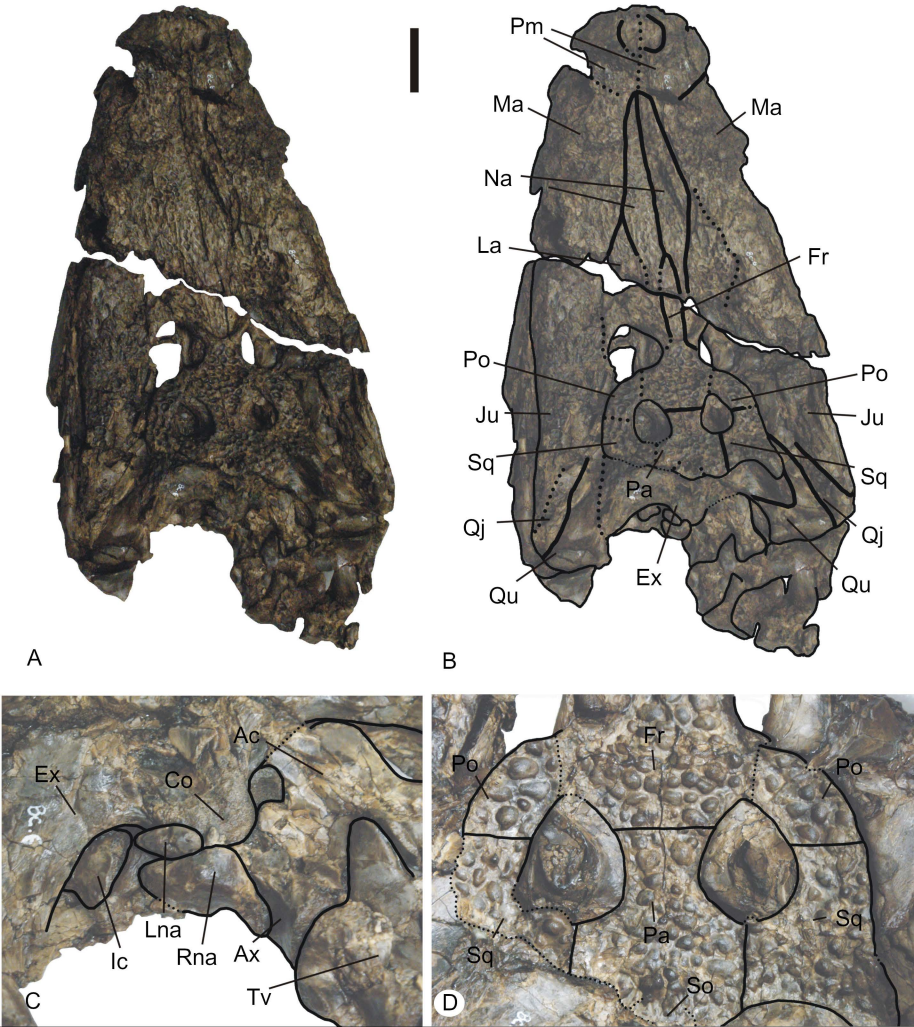
A
B
Pm
Ma
Ma
Na
La
Fr
Po
Po
Ju
Ju
Sq
Sq
Pa
Qj
Qj
Ex
Qu
Qu
C
Ac
Ex
Co
Lna
Ic
Rna
Ax
Tv
D
Fr
Po
Po
Sq
Pa
Sq
So

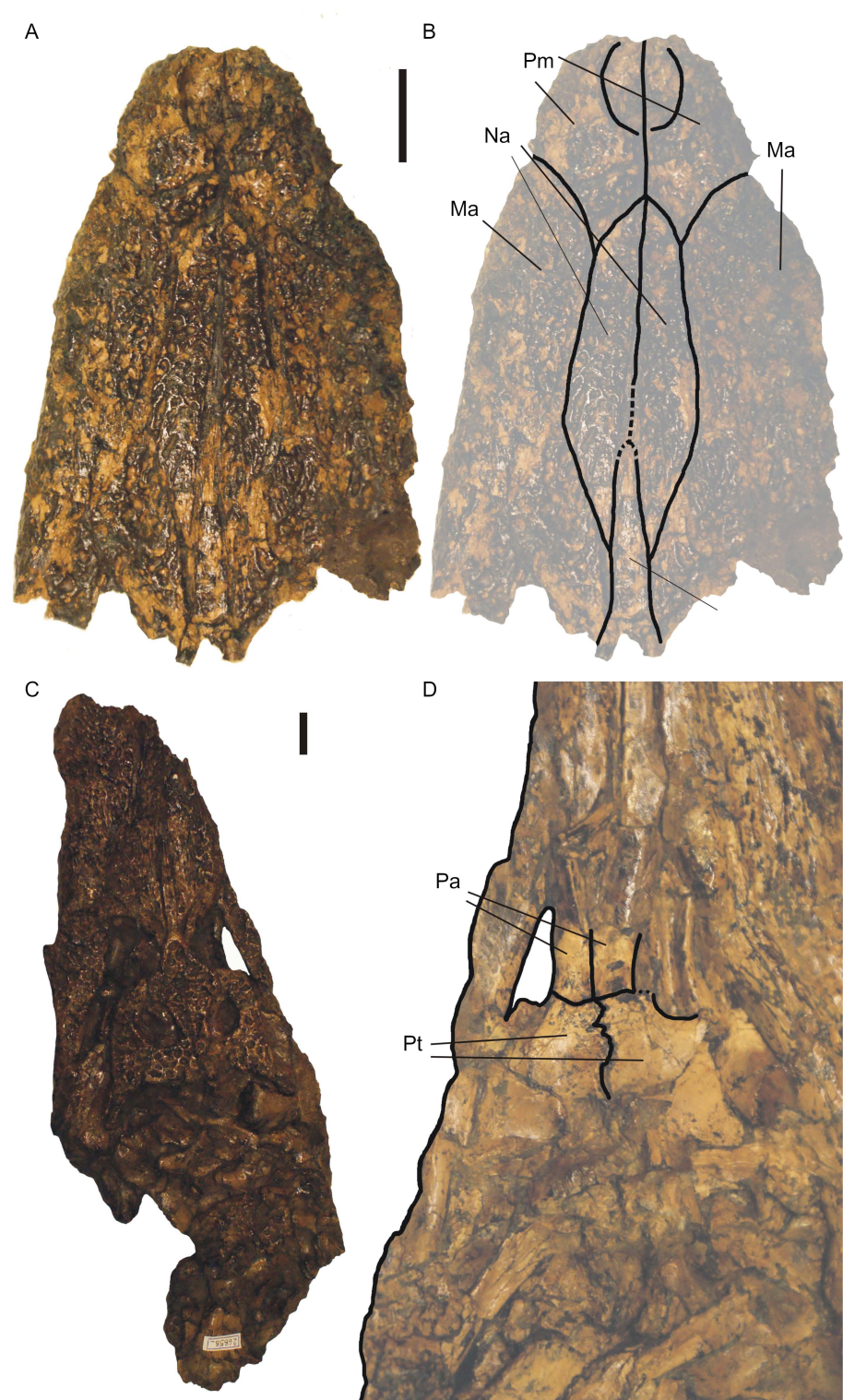
A
B
Pm
Na
Ma
Ma
C
D
Pa
Pt

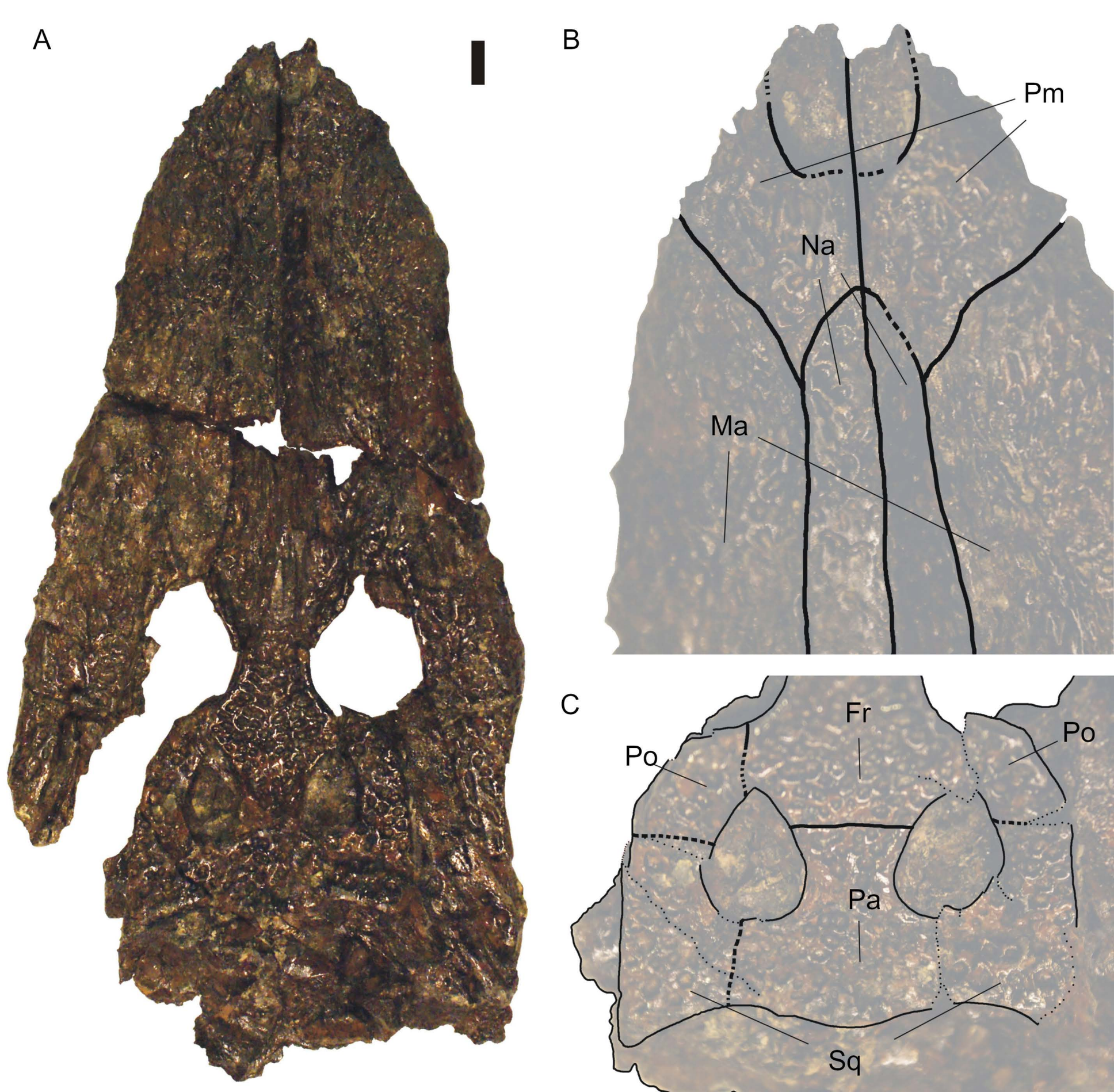
A
B
Pm
Na
Ma
C
Fr
Po
Po
Pa
Sq

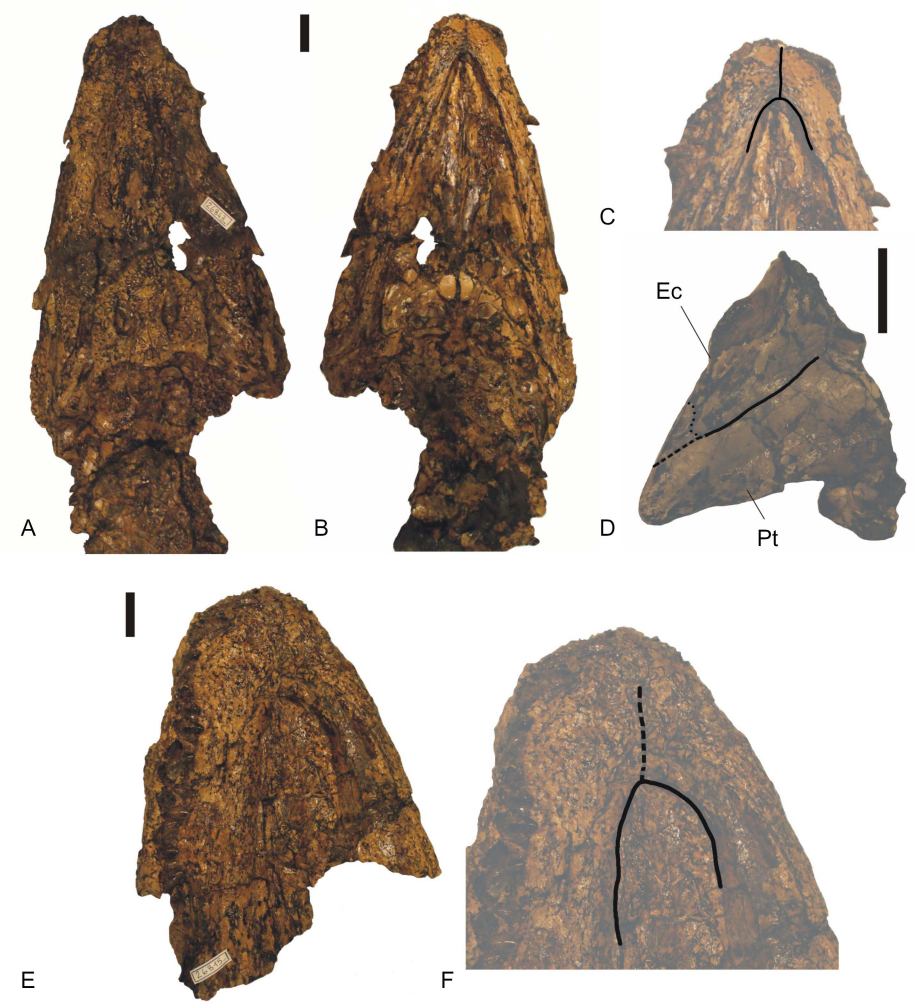
A
B
C
D
Ec
Pt
E
F

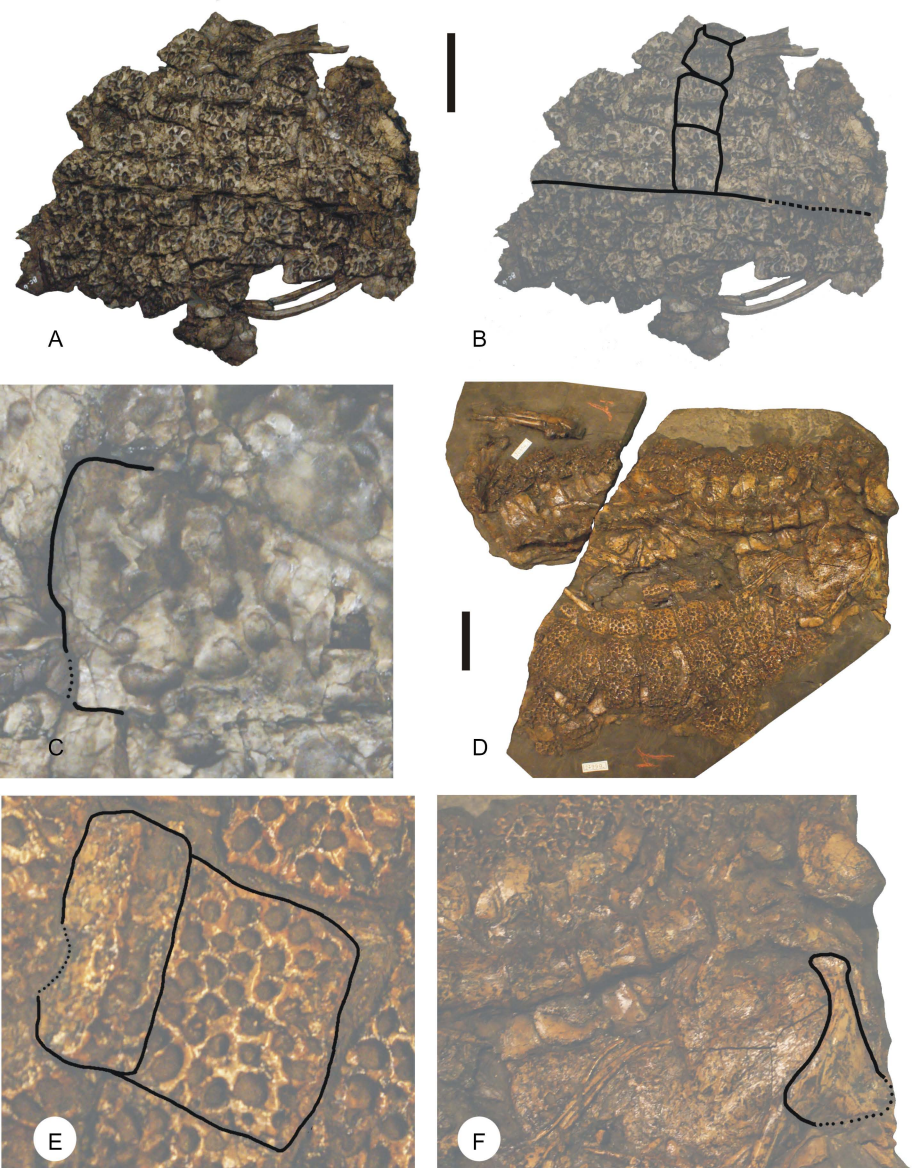
A
B
C
D
E
F

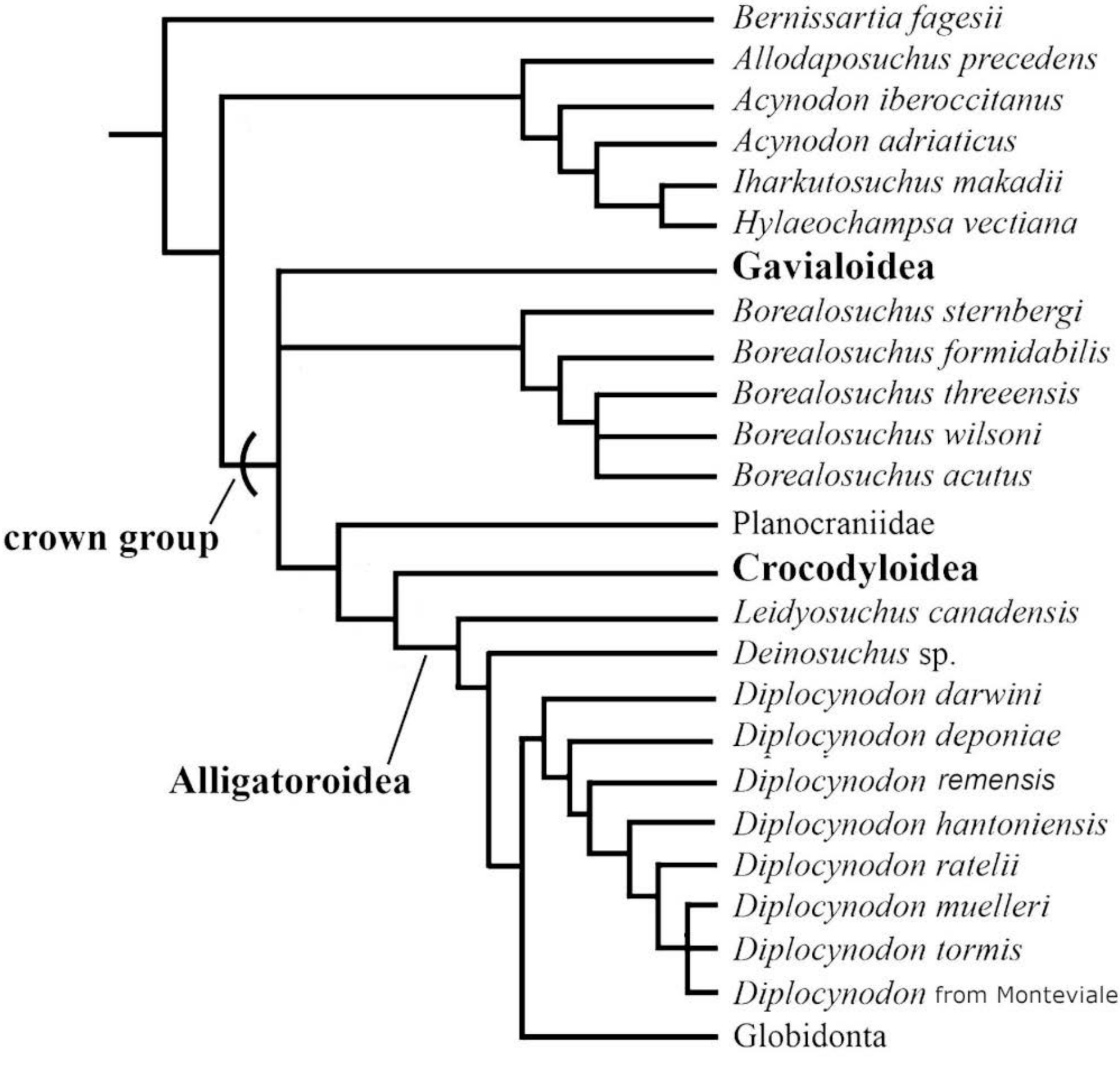
Bernissartia fagesii
Allodaposuchus precedens
Acynodon iberoccitanus
Acynodon adriaticus
Iharkutosuchus makadii
Hylaeochampsa vectiana
Gavialoidea
Borealosuchus sternbergi
Borealosuchus formidabilis
Borealosuchus threeensis
Borealosuchus wilsoni
Borealosuchus acutus
crown group
Planocraniidae
Crocodyloidea
Leidyosuchus canadensis
Deinosuchus sp.
Diplocynodon darwini
Diplocynodon deponiae
Alligatoroidea
Diplocynodon remensis
Diplocynodon hantoniensis
Diplocynodon ratelii
Diplocynodon muelleri
Diplocynodon tormis
Diplocynodon from Monteviale
Globidonta